

ADAPT: A Pseudo-labeling Approach to Combat Concept Drift in Malware Detection

1st Md Tanvirul Alam
Rochester Institute of Technology
Rochester, NY, USA
ma8235@rit.edu

2nd Aritran Piplai
University of Texas El Paso
El Paso, TX, USA
apiplai@utep.edu

3rd Nidhi Rastogi
Rochester Institute of Technology
Rochester, NY, USA
nxrvse@rit.edu

Abstract—Machine learning models are commonly used for malware classification; however, they suffer from performance degradation over time due to concept drift. Adapting these models to changing data distributions requires frequent updates, which rely on costly ground truth annotations. While active learning can reduce the annotation burden, leveraging unlabeled data through semi-supervised learning remains a relatively underexplored approach in the context of malware detection. In this research, we introduce ADAPT, a novel pseudo-labeling semi-supervised algorithm for addressing concept drift. Our model-agnostic method can be applied to various machine learning models, including neural networks and tree-based algorithms. We conduct extensive experiments on five diverse malware detection datasets spanning Android, Windows, and PDF domains. The results demonstrate that our method consistently outperforms baseline models and competitive benchmarks. This work paves the way for more effective adaptation of machine learning models to concept drift in malware detection.

Index Terms—malware detection, concept drift, semi-supervised learning, pseudo-labeling

I. INTRODUCTION

The ever-evolving nature of malware poses ongoing challenges to cybersecurity. Machine learning has been widely adopted for malware detection across various platforms, offering significant improvements over traditional signature-based and rule-based methods [8], [13], [36], [49], [52]. However, the effectiveness of these models is predicated on the assumption that the statistical properties of the training data remain stable over time [18]. In practice, this assumption rarely holds due to the dynamic nature of malware and the continuous evolution of underlying platforms, which introduce new features, APIs, and programming practices [38]. This leads to the problem of *concept drift*—a shift in the underlying data distribution that results in a significant degradation in model performance, necessitating constant monitoring and adaptation [43], [50].

Dealing with concept drift in malware detection is a multifaceted challenge. One approach aims to design inherently more drift-resistant systems by creating more robust feature spaces [49], [77]. However, concept drift remains inevitable due to the dynamic nature of the problem landscape, and it is unclear whether a malware representation immune to concept drift can be developed [15]. Another approach to addressing concept drift is periodic model retraining [46], [50]. Effective retraining first requires detecting when the model has become outdated, which triggers the need for an update [15], [37], [73].

Since retraining requires access to manually labeled drifted samples, active learning has been widely used to reduce the annotation effort [23], [47]. However, obtaining high-quality annotations for malware remains challenging, constituting a significant portion of the overall costs of developing an ML model, especially given the sheer volume of emerging malware variants [19], [45].

Self-training provides an alternative approach for concept drift adaptation without requiring additional annotations beyond the initial training data [7]. Pseudo-labeling is a learning paradigm where the model generates labels for unlabeled data, treating its predictions as ground truth to train itself [40], [57] further. A notable application of this approach for malware detection is DroidEvolver [70], which employs pseudo-labeling for Android malware detection by using an ensemble of online learning algorithms to eliminate labeling costs after the initial training phase. However, a later study [38] revealed that when experimental biases, such as unrealistic benign-to-malware ratios in the dataset, are addressed, DroidEvolver’s performance deteriorates significantly due to confirmation bias [12] and a catastrophic self-poisoning effect, leading to a sudden and severe performance drop. While the work in [38] proposed an enhanced version of DroidEvolver to mitigate these issues, the performance still deteriorates rapidly after a short period when solely relying on pseudo-labels. Thus, designing an effective pseudo-labeling-based approach for malware detection under concept drift remains a significant challenge.

In this work, we propose ADAPT: Adaptive Drift-aware Algorithm using Pseudo-labeling for malware detection, a semi-supervised learning approach tailored for concept drift in malware detection. Unlike general-purpose methods, ADAPT accounts for the asymmetric nature of drift, which predominantly affects malware rather than benign samples [15], [26]. We introduce a drift-aware pseudo-labeling strategy that selectively propagates labels based on class-specific drift behavior. Data augmentation plays a crucial role in the success of semi-supervised learning algorithms [17], [59]. While well-established in domains such as image classification [27], data augmentation techniques are relatively rare in malware classification. Nevertheless, prior work has shown promising results using data augmentation in noisy label settings for malware classification [69]. We extend this approach to the concept drift scenario, where the model is periodically retrained. To

further improve robustness, we incorporate mixup regularization [64], [74], which helps mitigate self-poisoning by improving confidence calibration. This is particularly important for our pseudo-labeling strategy, as it ensures that predicted probabilities reflect the actual likelihood of correctness more accurately.

We evaluate ADAPT on five diverse malware detection datasets—two Android, two Windows, and one PDF—and show that it consistently outperforms competitive semi-supervised learning methods, achieving state-of-the-art results across all tasks. We also demonstrate its effectiveness in an active learning setting, where ADAPT surpasses prior state-of-the-art performance on Android malware detection under the same annotation budget.

Our key contributions are:

- 1) We introduce ADAPT, a semi-supervised learning algorithm tailored for concept drift in malware detection. It mitigates catastrophic self-poisoning through drift-aware pseudo-labeling.
- 2) Our method is model-agnostic and shows improvements across Random Forest, XGBoost, and neural networks. We validate its effectiveness on five real-world malware datasets exhibiting varying degrees of concept drift.
- 3) We extend ADAPT to an active learning setting, achieving state-of-the-art results on Android malware detection. We also apply it to the multiclass problem of malware family classification and demonstrate its effectiveness under concept drift.

II. BACKGROUND AND RELATED WORK

A. Malware Detection using Machine Learning

Machine learning has been widely applied to malware detection [8], [13], [24], [42], [49], [77], both in academic research and industrial settings. These models are trained using features extracted through static analysis, dynamic analysis, a combination of both, or memory-based analysis [58]. Static features are obtained by analyzing the binary or source code of a file without executing it, making them a popular choice for malware detection [8], [13], [49]. While machine learning detectors built upon static features often achieve high performance when the training and test datasets follow the same distribution, their effectiveness deteriorates in real-world scenarios due to distributional changes caused by code obfuscation, concept drift, and adversarial examples [29]. In particular, concept drift, also known as dataset shift, is the primary focus of this study.

B. Concept Drift

Dataset shift refers to the phenomenon in machine learning where the joint distribution of inputs and outputs differs between the training and test stages [51]. Dataset shifts can be broadly categorized into three types: covariate shift, label shift, and concept shift. Covariate shift occurs when the distribution of the features, $p(x)$, changes. Label shift, also known as prior probability shift, refers to a change in the distribution of the labels, $p(y)$. Concept shift refers to a change

in the conditional probability distribution, $p(y|x)$, meaning the relationship between the features and the target labels changes, effectively altering the class definitions. The individual effects of these shifts can be challenging to disentangle from a finite set of samples [15], [51]. Consequently, in machine learning for security, it is common practice to refer to all these shifts under the broader term *concept drift* [15], [37], [38], which is the terminology we adopt in this work.

Concept drift in malware detection arises from both benign and malicious changes. While API updates and new functionalities in benign apps contribute to drift, the primary driver is the evolving behavior of malware [25], [77]. Adversaries continually adapt through obfuscation, packing, and novel attack strategies to evade detection [1], [9], [62]. These shifts alter the distribution of malicious behavior between training and testing data [15], leading to degraded classifier performance and reduced detection rates over time [5], [37], [50].

C. Concept Drift Adaptation

While developing feature spaces that are inherently more resilient to concept drift is an effective approach [49], [77], the dynamic nature of malware makes it challenging to design such feature spaces that remain effective over long periods [15]. As a result, machine learning models trained on these features need to be periodically retrained to stay functional.

Approaches like Transcend [37] and Transcendent [15] tackle drift through classification with rejection, using conformal evaluators to flag uncertain samples for expert review. However, the reliance on manual labeling limits retraining frequency due to cost and resource constraints [45], [70]. To address this, active learning has been used to reduce annotation effort by selectively labeling uncertain samples [23], [72], with studies showing up to 8x reduction in labeling cost [23]. More recently, pseudo-labeling has emerged as a promising alternative, enabling model updates without new annotations [38], [70]. Our research focuses on this setting; however, we also consider the active learning scenario in Section VIII.

D. Pseudo-Labeling for Drift Adaptation

Pseudo-labeling is a technique that leverages model predictions to assign labels to unlabeled data, assuming that predictions with high confidence are likely to be accurate. These pseudo-labels are then incorporated into the training process, enabling the model to learn from labeled and unlabeled samples. Pseudo-labeling is widely used in semi-supervised learning setups [17], [59]. However, in the context of malware detection, its application typically does not account for adapting to concept drift [44], [48], [56], [69].

DroidEvolver [70] applies pseudo-labeling for Android malware detection under concept drift using an ensemble of linear models and online learning to avoid manual labeling. However, it was later shown to underperform when accounting for dataset biases [38], prompting several improvements. More recent work includes MORPH [3], which uses neural networks but suffers from high false positive rates, and Insomnia [10],

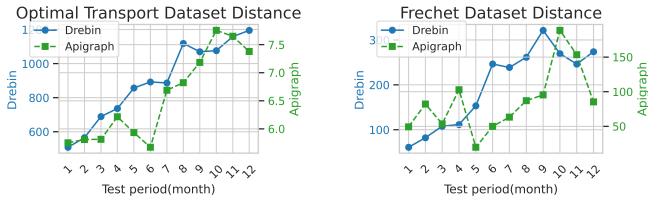


Fig. 1: Impact of covariate shift $p(x)$ and concept shift $p(y|x)$ on the first year of the test set for the two Android datasets, evaluated using Optimal Transport Dataset Distance and Fréchet Distance.

which applies co-training for drift adaptation in network intrusion detection.

Despite its potential, pseudo-labeling under concept drift poses challenges: as distributions shift, model predictions become less reliable, leading to incorrect pseudo-labels and self-reinforcing errors—known as self-poisoning [12], [38]. In this work, we propose a pseudo-labeling approach specifically designed to mitigate these effects.

III. RESEARCH MOTIVATION

a) Nature of Concept Drift in Malware Detection:

While it is not feasible to precisely measure different forms of dataset shift from a finite set of samples, these shifts can be approximated using various metrics. In this work, we use the Optimal Transport Dataset Distance (OTDD) [6] to approximate covariate shift and the Fréchet Dataset Distance (FDD) [35] to approximate concept shift, following the methodology suggested in [31].

OTDD [6] measures the distance between two distributions by computing the minimum cost of transforming one distribution into another, leveraging optimal transport theory. Using a Gaussian approximation, we calculate the OTDD between the first year of testing data and the original training data. This distance is computed directly in the feature space without relying on a trained model.

Fréchet Dataset Distance (FDD) [35], initially used in generative models, measures the similarity between two distributions by comparing their intermediate feature representations in a reference classifier. To compute the FDD, we use the MLP model trained with the best hyperparameters (as described in Section VI-C). Specifically, we take the penultimate layer features of the trained model for each month's samples and compare them with the features from the training month to obtain the FDD. More details on these metrics can be found in their respective papers [6], [35].

The results for the two Android malware detection datasets used in this study are shown in Figure 1. The magnitude of both covariate and concept shift is higher in the Drebin [13] dataset compared to APIGraph [77], as APIGraph employs a more compact feature space that captures semantically similar API calls. The general trend shows that these shifts gradually increase in both datasets. In particular, these shifts lead to poorer malware detection performance when the model is not

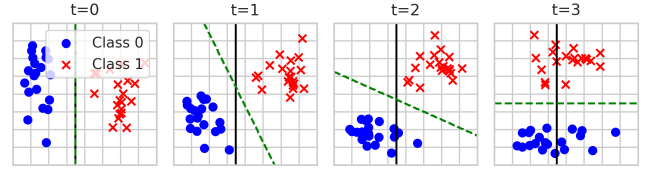


Fig. 2: Adaptation to distribution shift for a binary classifier. The solid line represents the original classifier, and the dotted lines represent the adapted classifier trained with pseudo-labels.

updated. This highlights that malware detection datasets often exhibit different shifts, which can interact in complex ways to degrade classifier performance.

b) *Self-training for drift adaptation*: Self-training with pseudo-labeling can allow a model to adapt to evolving data distributions without requiring continuous manual labeling [39]. This process is illustrated in Figure 2 using a 2D toy dataset with a logistic regression classifier. In this example, both $p(x)$ and $p(y|x)$ gradually change from $t = 0$ to $t = 3$, with the dataset undergoing continuous rotation. As a result, the classifier's initial decision boundary (solid line) misclassifies most samples by $t = 3$.

However, by using the model's own predictions as pseudo-labels and retraining on these pseudo-labeled samples, the model can adapt to the changing data distribution. The updated classifier (dashed line) in Figure 2 successfully separates the dataset at the intermediate stages and in the final step. While this example demonstrates the effectiveness of self-training in a simple, idealized scenario, real-world malware datasets are significantly more complex. A naive application of pseudo-labeling in these cases can lead to performance degradation [38].

Nevertheless, malware datasets typically undergo gradual distributional shifts, as illustrated in Figure 1, where both covariate and concept shifts increase over time. Based on this observation, we hypothesize that an effective self-training approach can continuously adapt the model to account for these evolving shifts. Notably, prior work by Kumar et al. [39] establishes formal error bounds of self-training under the assumption of gradual distributional shifts. Our method builds on this foundation by extending their framework, and we provide a rigorous theoretical analysis in Appendix K.

IV. PROPOSED METHOD

We introduce ADAPT, a pseudo-labeling-based self-training algorithm for handling concept drift in malware detection. ADAPT is compatible with various learning algorithms, including tree-based methods and neural networks. We evaluate three baseline models in our experiments: Random Forest (RF), XGBoost, and Multilayer Perceptron (MLP). These models were selected because different algorithms may perform better on different datasets, and simpler models like Random Forest can be preferable due to their efficiency in specific applications [2], [28], [37], [60], [72].

Algorithm 1 ADAPT: Adaptive Drift-aware Algorithm using Pseudo-labeling for malware detection

```

1: Input: Labeled dataset  $\mathcal{D}_l$ , unlabeled dataset  $\mathcal{D}_u$ 
2: Output: Updated model  $M$ 
3: Train initial model  $M_0$  on the labeled dataset  $\mathcal{D}_l$ 
4: for each test month from  $i = 1$  to  $T$  do
5:   Step 1: Pseudo-Label Selection
6:   Select pseudo-labeled samples:  $\mathcal{D}_p = \{(x_i, \hat{y}_i)\}$  from
     the unlabeled dataset  $\mathcal{D}_u$  using the model  $M_{i-1}$  [see
     §IV-A].
7:   Merge the labeled and pseudo-labeled data:  $\mathcal{D}_m = \mathcal{D}_l \cup \mathcal{D}_p$ 
8:   Step 2: Data Augmentation
9:   Apply data augmentation to  $\mathcal{D}_m$  to generate the aug-
     mented dataset  $\mathcal{D}_{\text{aug}}$  [§IV-B].
10:  Step 3: Mixup Regularization
11:  Apply mixup regularization on  $\mathcal{D}_m$  to produce the
     mixup-augmented dataset  $\mathcal{D}_{\text{mixup}}$  [§IV-C].
12:  Step 4: Model Retraining
13:  Combine the merged, augmented, and mixup datasets:
      $\mathcal{D}_{\text{combined}} = \mathcal{D}_m \cup \mathcal{D}_{\text{aug}} \cup \mathcal{D}_{\text{mixup}}$ 
14:  Retrain the model  $M_i$  for the current month on the
     combined dataset  $\mathcal{D}_{\text{combined}}$ 
15: end for

```

We assume that we initially have access to an annotated, labeled dataset. Specifically, we are given a set of N annotated samples with features $\{x_1, x_2, \dots, x_N\}$ and their corresponding binary labels $\{y_1, y_2, \dots, y_N\}$, where 0 represents a benign sample and 1 represents malware. We first train a supervised machine learning model, denoted as M_0 , using this labeled data. We later extend our analysis to the multiclass setting, which is discussed in Section IX.

After the initial training, the model is periodically updated each subsequent month using unlabeled test data. This experimental setting aligns with prior work on concept drift adaptation, such as the approach by Chen et al. [23] for continuous learning. We employ our proposed algorithm during each monthly retraining period to leverage the unlabeled data, improving the model’s ability to adapt to concept drift.

ADAPT comprises four key steps during the semi-supervised update phase:

- 1) **Adaptive Drift-Aware Pseudo-Labeling:** In this step, we select model predictions that are eligible for inclusion in the self-training process. We propose a novel adaptive pseudo-label selection method to improve the label quality of the selected samples. Details of the pseudo-labeling method are provided in Section IV-A.
- 2) **Data Augmentation with Label Consistency:** To increase the diversity of the training data, we apply a data augmentation phase. Augmentation has proven to be an effective strategy in self-training and semi-supervised learning, especially in scenarios like malware classification where labels can be noisy. The specifics of our augmentation technique are discussed in Section IV-B.

- 3) **Confidence Calibration with Mixup:** High-quality pseudo-labels are crucial for successful self-training. Poor pseudo-labels can lead to issues such as self-poisoning, where the model reinforces its incorrect predictions, and confirmation bias. Since we use confidence thresholding to filter out low-confidence predictions, it is essential to calibrate the model’s confidence levels—i.e., to ensure that predictions with high confidence are indeed more likely to be correct. To achieve this, we integrate the mixup [75] regularization technique, which has been shown to improve model calibration in prior work [64]. Further details on the mixup method are provided in Section IV-C.
- 4) **Model Retraining:** In the final step, we combine the original labeled data, the pseudo-labeled data, and the datasets generated through augmentation and mixup regularization. The model is then updated on this combined dataset. For traditional models like random forests and XGBoost, we retrain the model from scratch, while for neural networks, we fine-tune the model, following the guidelines in [23].

Algorithm 1 provides an overview of the ADAPT algorithm.

A. Adaptive Drift-Aware Pseudo-Labeling

In traditional pseudo-label selection, a fixed threshold τ is used to filter out low-confidence predictions [40]. Given a model M and its predicted probability for a sample \mathbf{x}_j , the pseudo-label \tilde{y}_j is defined as:

$$\tilde{y}_j = \begin{cases} \arg \max_k \hat{y}_j^{(k)}, & \text{if } \max_k \hat{y}_j^{(k)} \geq \tau, \\ \text{unlabeled}, & \text{otherwise.} \end{cases}$$

Here, $\hat{y}_j^{(k)}$ denotes the predicted probability of the k -th class for the unlabeled sample \mathbf{x}_j . This formulation assumes that the model outputs probabilities for two classes, benign and malware, which sum to 1. If the model instead outputs only the probability p_1 for the positive (malware) class—such as in the case of a neural network with a single output neuron and sigmoid activation—then the probability for the benign class is $p_0 = 1 - p_1$. In either case, if the predicted probability for the assigned class exceeds the predefined threshold τ , the sample is pseudo-labeled; otherwise, it remains unlabeled.

Using a fixed thresholding approach for malware detection has limitations due to the divergent drift patterns in the benign and malware classes, as shown in Figure 3. In this figure, we plot the average prediction probability for the benign and malware classes using the XGBoost and MLP models on the Android datasets. The malware class experiences more severe drift, as indicated by its consistently lower average prediction probability than the benign class.

To address this, we propose a class-dependent adaptive thresholding strategy for pseudo-label selection, which dynamically adjusts to the evolving data distribution. While dynamic thresholding has been applied in other domains [67], these approaches do not consider the distinct nature of drift across different classes. In our method, we define separate thresholds for the two classes: $\tau_m \in [0.5, 1]$ for malware and $\tau_b \in [0.5, 1]$ for benign samples. The adaptive thresholding mechanism

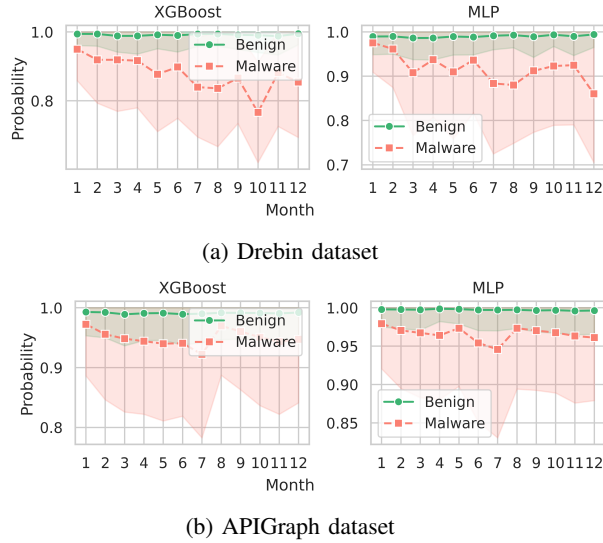


Fig. 3: Mean and standard deviation of predicted probabilities for benign and malware classes using XGBoost and MLP models on two datasets. Malware predictions typically have lower confidence, indicating concept drift primarily affects the malware class.

adjusts these thresholds based on the model’s average prediction probabilities for each class over the unlabeled data. Specifically, we compute the mean probability for each class as follows:

$$\mu_m = \frac{1}{|\mathcal{D}_u^m|} \sum_{x_j \in \mathcal{D}_u^m} P(y = 1 | x_j) \quad (1)$$

$$\mu_b = \frac{1}{|\mathcal{D}_u^b|} \sum_{x_j \in \mathcal{D}_u^b} P(y = 0 | x_j) \quad (2)$$

where \mathcal{D}_u^m and \mathcal{D}_u^b represent the subsets of the unlabeled dataset \mathcal{D}_u that are predicted as malware and benign by the model M , respectively. The quantities μ_m and μ_b are the mean probabilities for the malware and benign classes. While in our experimental setup, these values are computed using all the samples from the current month’s data, the formulation can also be applied in a batch or online learning setting, where the quantities are computed based on batch statistics of the model’s predicted pseudo-labels.

We then combine these mean probabilities with the prior thresholds τ_m and τ_b using a parameter $\lambda \in [0, 1]$ to compute the updated thresholds, which accounts for the gradual shift in the data:

$$\tau_m^{\text{updated}} = \lambda \cdot \mu_m + (1 - \lambda) \cdot \tau_m \quad (3)$$

$$\tau_b^{\text{updated}} = \lambda \cdot \mu_b + (1 - \lambda) \cdot \tau_b \quad (4)$$

After updating the thresholds, pseudo-labeled data is selected using these new adaptive thresholds. Specifically, if the model’s predicted probability for a sample exceeds the updated threshold for malware (τ_m^{updated}), the sample is assigned a label of 1 (malware). If the probability exceeds the updated

threshold for benign (τ_b^{updated}), it is labeled as 0 (benign). Otherwise, the sample remains unlabeled. Formally:

$$\hat{y}_j = \begin{cases} 1, & \text{if } P_M(y = 1 | x_j) > \tau_m^{\text{updated}} \\ 0, & \text{if } P_M(y = 0 | x_j) > \tau_b^{\text{updated}} \\ \text{unlabeled}, & \text{otherwise} \end{cases}$$

The values of the threshold parameters τ_m and τ_b , as well as the adaptation parameter λ , are jointly optimized during hyperparameter tuning, along with other model parameters, as discussed in Section VI-C.

B. Data Augmentation with Label Consistency

Data augmentation is a commonly used technique in semi-supervised learning, particularly in contrastive learning, where the model is encouraged to produce consistent predictions for a sample and its perturbed counterpart [17], [59]. While data augmentation methods are prevalent in domains like computer vision, this is not the case for malware detection. In image classification, various label-preserving transformations, such as rotation, translation, scaling, and flipping, can be easily applied [27]. However, designing equivalent transformations for malware datasets is significantly more challenging. Malware datasets typically consist of hand-crafted features, making it difficult to determine whether random transformations in the feature space preserve both the functionality and maliciousness of the application.

To address this challenge, Wu et al. [69] proposed a data augmentation strategy for Windows malware classification in which features are randomly masked and replaced with features from other samples in the dataset. Given a sample $\mathbf{x} \in \mathbb{R}^d$, a mask vector $\mathbf{m} = [m_1, \dots, m_d]^T \in \mathbb{R}^d$ is first generated, where each m_j is independently sampled from a Bernoulli distribution with probability p_a . The augmented sample $\tilde{\mathbf{x}}$ is then obtained using the following equation:

$$\tilde{\mathbf{x}} = (1 - \mathbf{m}) \odot \hat{\mathbf{x}} + \mathbf{x} \odot \mathbf{m} \quad (5)$$

where \odot denotes element-wise multiplication, and $\hat{\mathbf{x}}$ is a new sample where each feature \hat{x}_i is sampled from the empirical marginal distribution of the i -th feature. This empirical marginal distribution is represented by the uniform distribution over the values that the feature takes across the entire training dataset.

For example, consider a dataset with three features and four samples:

$$\{[0, 1, 0], [1, 1, 0], [0, 0, 1], [0, 1, 1]\}.$$

The value of the second feature of $\hat{\mathbf{x}}$ would be randomly sampled from the set $\{1, 1, 0, 1\}$, which are the observed values of the second feature across all samples.

While the data augmentation strategy proposed by Wu et al. [69] was designed for semi-supervised learning in a static setting where the model is trained only once, our scenario involves multiple model updates with additional pseudo-labeled data. Data augmentation can introduce samples whose labels may change due to concept drift in this setting. Such label flipping can degrade model performance in subsequent stages.

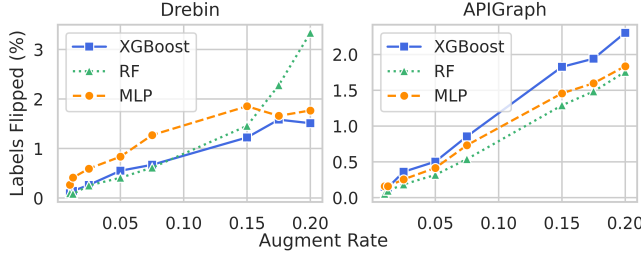


Fig. 4: Percentage of samples in the Drebin and APIGraph datasets where augmentation causes the model’s originally correct prediction to flip (i.e., benign to malicious or malicious to benign).

We illustrate this effect in Figure 4 using the Drebin and APIGraph datasets across different models. Specifically, we select samples from the validation set where the model’s original prediction is correct and apply augmentation with varying masking probabilities. We then recompute the model’s predictions on the augmented data. Since augmentation should not alter the ground truth, if the model’s prediction changes and becomes incorrect, we classify this as a case of label flipping. As the strength of the augmentation increases, the proportion of samples experiencing label flipping also rises. This suggests that overly strong augmentations can cause samples to cross the model’s decision boundary, introducing additional noise into the learning process, which can accumulate over time.

To address this, we propose two key modifications to ensure label consistency during augmentation. First, when replacing a masked feature, we restrict the replacement values only from samples of the same class. Although this setting was considered in [69], we argue that preserving label consistency is even more critical in our iterative training framework. Second, after the initial training phase, we leverage the current model to predict the label of the augmented sample. The augmented sample is included in the dataset only if the model’s prediction matches the original label to improve label consistency. However, it is important to note that feature consistency is not explicitly enforced during augmentation. This means the generated features may not always represent valid samples, potentially leading to inconsistencies. We explore this issue in more detail in Appendix J.

C. Confidence Calibration with Mixup

One of the key challenges with self-training is the issue of confirmation bias (also referred to as self-poisoning), where the model reinforces its incorrect predictions [12]. This occurs when the model makes an incorrect prediction, uses that prediction to update itself, and consequently becomes more confident in that incorrect prediction in future iterations.

Pseudo-labeling methods rely on thresholding to filter out low-confidence predictions and retain only high-confidence predictions. This process assumes that higher-confidence predictions are more likely to be correct. However, this as-

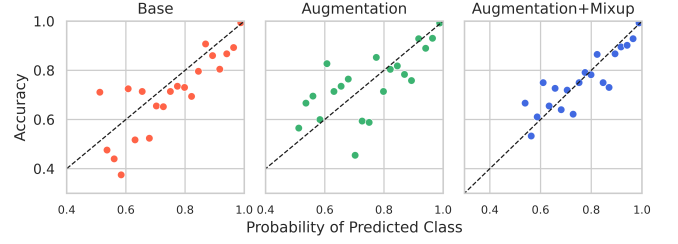


Fig. 5: APIGraph dataset

Fig. 6: Calibration plots for the XGBoost model on the APIGraph dataset. The model trained with Mixup shows better calibration, as the points are lying closer to the $y = x$ line.

sumption may not always hold due to issues with confidence calibration—the model’s predicted confidence may not always reflect the true likelihood of the prediction being correct. By improving the model’s confidence calibration, we can ensure that the pseudo-labels we incorporate into training are more accurate, thereby reducing the impact of self-poisoning.

To address this, we use *mixup* [74], a regularization technique to improve model generalization and calibration. Mixup generates new training samples by interpolating both features and labels between two randomly selected samples. Specifically, given two samples, the features and labels are mixed based on a mixing coefficient λ drawn from a Beta distribution parameterized by α . This results in fractional labels when mixing samples from different classes. As shown in [64], label interpolation is crucial for improving calibration. The target labels become fractional instead of one-hot, which changes the loss function for neural networks to the following:

$$\mathcal{L}_{\text{mixup}} = \lambda \cdot \mathcal{L}(y_i, \hat{y}_i) + (1 - \lambda) \cdot \mathcal{L}(y_j, \hat{y}_i)$$

where \mathcal{L} is the binary cross-entropy loss, y_i and y_j are the true labels, and \hat{y}_i is the model’s prediction.

However, this approach is not applicable to models like Random Forests, which do not support fractional targets for classification tasks. To handle this, when mixing two samples with different labels, we assign the label corresponding to the sample with the higher interpolation coefficient.

We demonstrate the effectiveness of Mixup in improving model calibration in Figure 6 using the XGBoost model on the APIGraph dataset. The scatter plots illustrate the model’s accuracy versus its confidence for different confidence bins across three models: the base model trained without data augmentation or Mixup (left), the model trained with only data augmentation (middle), and the model trained with both Mixup and data augmentation (right), all evaluated on the validation dataset. A well-calibrated model will have most points close to the $y = x$ line, indicating that the model’s confidence aligns with its actual accuracy. The figure shows that the base model exhibits significant overconfidence, where its confidence exceeds its true accuracy. This overconfidence can be particularly problematic when using thresholds to select pseudo-labeled samples. In contrast, the model trained with data augmentation shows improved calibration, and the

TABLE I: Summary statistics of the datasets

Dataset	Split	Duration	Benign Apps	Malicious Apps
Drebin	Train	2019-01 to 2019-12	21449	2187
	Validation	2020-01 to 2020-06	10549	777
	Test	2020-07 to 2021-12	20106	822
APIGraph	Train	2012-01 to 2012-12	16194	1447
	Validation	2013-01 to 2013-06	13769	1446
	Test	2013-07 to 2018-12	175048	13895
BODMAS	Train	2019-10 to 2019-12	13763	11082
	Validation	2020-01 to 2020-03	13206	13769
	Test	2020-04 to 2020-09	32608	27701
EMBER	Train	2018-01	29423	32040
	Validation	—	—	—
	Test	2018-02 to 2018-12	320577	358864
PDF	Train	10/13 to 10/27	25233	1208
	Validation	10/27 to 09/10	70041	1893
	Test	09/10 to 10/22	135751	20224

model trained with both Mixup and data augmentation further enhances this, with its confidence more accurately reflecting its accuracy, especially in high-confidence regions.

V. DATASETS

We evaluate ADAPT across five publicly available malware detection datasets: two Android malware datasets, two Windows PE malware datasets, and one PDF malware dataset. Although the two Windows datasets share the same feature representation, they cover different time periods. The Android datasets differ both in feature sets and collection timelines. Table I summarizes key statistics for each dataset.

A. Android Datasets

We use two Android malware detection datasets introduced by Chen et al. [23] for continuous learning using static features. The first dataset utilizes the Drebin feature set [13], while the second employs the APIGraph feature set [77].

The Drebin and APIGraph datasets represent Android applications using binary feature vectors that indicate the presence or absence of specific attributes. Drebin includes 16,978 dimensional features spanning eight categories: permissions, intents, API usage, and network addresses. In contrast, APIGraph reduces the feature space to 1,159 dimensions by clustering semantically similar APIs. Drebin samples were collected between 2019 and 2021, while APIGraph spans from 2012 to 2018. Both datasets were curated to mitigate experimental bias in malware detection [50], though they originally contained duplicates, which can affect result consistency [2], [78]. We, therefore, use deduplicated versions of both datasets in our experiments.

For both datasets, we use the first year’s data as the training set, the next six months for validation, and the remaining months for testing. For pseudo-labeling, the training data is used to train the initial model, which is then periodically updated with data from subsequent months in the validation and test sets. The validation set is also used to jointly tune

the model’s hyperparameters and those specific to the pseudo-labeling algorithm.

B. Windows Datasets

We use two Windows PE malware datasets: EMBER [8] and BODMAS [72]. Both datasets share identical feature sets but span different periods. Each file’s features, extracted using the LIEF project [63], consist of byte sequences, imported functions, and header information compiled into a 2,381-dimensional feature vector.

Since both datasets have the same feature representation, we perform hyperparameter tuning only on the BODMAS dataset and use those tuned hyperparameters to evaluate the EMBER dataset. For the BODMAS dataset, we use the first three months of data for training, the next three months for validation, and the remaining six months for testing. For the EMBER dataset, we treat the first month’s data as the labeled training set and use the remaining months for testing.

C. PDF Dataset

We use the PDF malware dataset from [60] in our study. The dataset contains features representing benign and malicious PDFs over ten weeks, from 09/13/2012 to 10/22/2012. Although the number of features varies between weeks, we restrict our analysis to the features consistently present across all weeks to ensure compatibility with the model architectures used in our experiments. This results in 950-dimensional feature vectors. Compared to the Android and Windows datasets, this dataset exhibits less concept drift due to the shorter period.

For training, we randomly sample 10% of the data from the first two weeks. The following two weeks are used for validation, and the test set consists of data from the final six weeks.

VI. EXPERIMENTAL SETTINGS

A. Baseline Machine Learning Models

Our proposed algorithm is compatible with most machine learning models, requiring only access to model probabilities for pseudo-labeling, with data augmentation applied in a model-agnostic manner. We evaluate its performance using three widely adopted baseline models: Random Forest (RF) [20], XGBoost [22], and a Multi-Layer Perceptron (MLP) [55], chosen for their relevance in malware classification tasks [4], [8], [28], [50], [72], [77]. RF is computationally efficient, interpretable, and performs well on smaller datasets. XGBoost excels on tabular data, typical in malware detection, due to its ability to capture complex feature interactions [2], [33]. MLPs are well-suited for large-scale semi-supervised settings, supporting batch training and dynamic data augmentation, and exhibit robustness to noisy labels [69], making them ideal for pseudo-labeling methods [59].

B. Self-Training Baselines

We compare our method against four self-training baselines: Adaptive Random Forest (ARF) [32], DroidEvolver++ (DE++) [38], Insomnia [10], and MORSE [69]. ARF and

DE++ are online learning methods that address concept drift without requiring access to the original training dataset. In contrast, Insomnia and MORSE follow a semi-supervised paradigm, leveraging the original training data and pseudo-labeled samples for model updates. While our approach (ADAPT) also assumes access to the original training data, we additionally explore scenarios where this access is restricted. Further implementation details for all baseline methods are provided in Appendix B, and the restricted setting without original training data is discussed in Appendix G.

C. Hyperparameter Tuning

As shown in previous works [2], [23], continuous learning settings require their own hyperparameter tuning. In our experiments, we perform joint hyperparameter tuning for the machine learning models and our proposed method using the validation set.

We introduce five hyperparameters in ADAPT: the benign base threshold τ_b , the malware base threshold τ_m , the threshold weight λ for adaptive thresholding, the masking probability for augmentation p_a , and the Mixup parameter α . Each baseline self training method has its own set of hyperparameters. Specifically:

- **ARF**: threshold τ
- **DE++**: app buffer size B , the ratio of malware to benign samples in the buffer m_r , and the threshold for model aging τ_a
- **Insomnia**: the fraction of samples considered for pseudo-labeling p_r
- **MORSE**: threshold τ , weak augmentation masking probability p_w , and strong augmentation masking probability p_s

A detailed list of model and self-training hyperparameters, along with their respective ranges, is provided in the Appendix L. Since different methods introduce varying numbers of hyperparameters, we use a fixed hyperparameter search budget to ensure a fair comparison between methods, as recommended in [2]. Specifically, we conduct 200 random hyperparameter searches [16] for each method on each dataset.

D. Evaluation

We use the same performance metrics as in [23]: the average F1-score, False Positive Rate (FPR), and False Negative Rate (FNR) across all months. Experiments are conducted using the optimal hyperparameters, with five random seeds on the test set. We report the mean and standard deviation of the performance metrics across these runs.

VII. RESULTS AND DISCUSSIONS

A. Drebin Dataset

Table II presents the results on the Drebin dataset for various methods. Drebin is the most challenging dataset, as reflected by the poor F1 scores of the offline machine-learning models. Among the four baselines, ARF, DE++, and MORSE fail to show notable improvement over the offline models. In contrast, Insomnia performs better than the offline MLP and XGBoost

TABLE II: Performance on the Drebin dataset.

Method		F1	FPR	FNR
Offline ML	RF	33.2±1.00	0.14±0.04	78.7±0.71
	XGBoost	44.9±0.00	0.66±0.00	65.6±0.00
	MLP	40.9±1.10	0.57±0.04	69.8±0.82
Self-Training	ARF	34.0±7.14	9.88±7.24	45.8±5.21
	DE++	34.7±1.89	7.84±1.17	47.1±3.08
	Insomnia	49.8±0.03	0.70±0.01	60.6±0.15
	MORSE	41.2±0.66	4.50±0.15	54.7±0.96
Proposed	RF+ADAPT	49.8±0.26	0.21±0.01	64.3±0.23
	XGBoost+ADAPT	57.1±0.37	0.24±0.04	56.6±0.37
	MLP+ADAPT	50.5±2.40	0.77±0.49	59.1±0.96

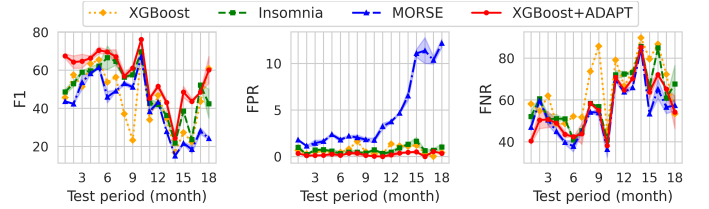


Fig. 7: Performance on the Drebin dataset: F1 score (left), FPR (middle), and FNR (right) over test months.

models, indicating that our adaptation of Insomnia for the training process is effective for Android malware detection under concept drift, even though Insomnia was originally designed for network intrusion detection.

Our proposed semi-supervised method shows considerable improvements across all baseline models. The absolute improvement in F1-score for RF, XGBoost, and MLP is 16.6%, 12.2%, and 9.6%, respectively. This improvement is primarily attributed to a significant reduction in false negatives (i.e., malware samples misclassified as benign). Notably, our method does not increase the false positive rate; in fact, it reduces the false positive rate by 63.6% compared to the baseline XGBoost model.

Figure 7 shows the F1 score over the test months for four different models on the Drebin dataset. Our proposed method consistently outperforms the other models across most test months. As evident from the figure, all three adaptation algorithms can mitigate the effects of concept drift to varying degrees.

B. APIGraph Dataset

The results for the APIGraph dataset are presented in Table III. The baseline machine learning models perform better on this dataset, as its features are designed to be more resistant to concept drift [77]. Among the baselines, three self-training models, excluding DE++, show improvements over the offline models.

Our proposed method demonstrates significant improvements over the baseline models, particularly for RF and MLP, both of which exhibit around 20% increase in F1-score. While MORSE achieves the best False Negative Rate, our method achieves a lower False Positive Rate with the best-performing MLP model.

TABLE III: Performance on the APIGraph dataset.

Method		F1	FPR	FNR
Offline ML	RF	46.8±3.89	0.34±0.08	66.9±3.76
	XGBoost	66.5±0.90	0.97±0.00	42.7±0.90
	MLP	57.0±3.52	1.67±0.64	49.9±6.78
Self-Training	ARF	61.1±5.84	5.28±3.68	25.0±10.8
	DE++	42.3±30.1	0.33±0.25	65.6±24.6
	Insomnia	68.1±0.43	2.05±0.10	31.8±1.00
	MORSE	<u>75.3±0.82</u>	1.82±0.23	22.2±0.77
Proposed	RF+ADAPT	67.2±0.29	0.34±0.01	46.0±0.36
	XGBoost+ADAPT	73.2±0.92	2.26±0.23	22.2±0.48
	MLP+ADAPT	76.8±0.52	0.81±0.10	29.4±0.97

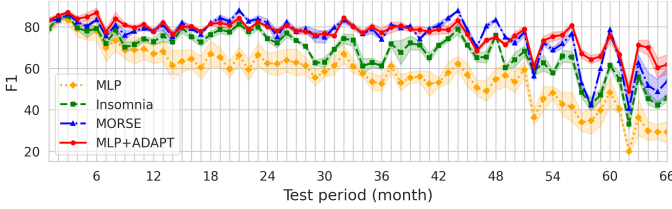


Fig. 8: F1-score over test months on APIGraph dataset.

Figure 8 shows the F1-score over the test months for four models on the APIGraph dataset. The performance of all three adaptation models remains relatively stable for the first two years of test data, after which Insomnia shows a sharp decline. Our proposed method and MORSE perform similarly for most of the test period, except towards the end, where more significant drift occurs, and our proposed method outperforms MORSE under these conditions.

C. Windows Datasets

a) **BODMAS dataset:** The results for the BODMAS and EMBER datasets are presented in Table IV and Table V, respectively. The baseline models achieve significantly higher F1 scores on these datasets, indicating a less pronounced impact of concept drift. The performance on the EMBER dataset is slightly lower, primarily because we did not perform separate hyperparameter tuning for this dataset and used only one month of data for training, compared to the three months used for BODMAS.

None of the self-training baseline methods on the BODMAS dataset outperform the baseline XGBoost model, which already achieves an F1-score of 99.2%. However, our proposed method improves this score by an additional 0.4%, with reductions in both the False Positive Rate (FPR) and False Negative Rate (FNR). This underscores the importance of our model-agnostic approach, as tree-based models may inherently perform better than neural networks on certain datasets [33]. A similar improvement is observed for MLP, although the performance of RF decreases—a trend that is also consistent with the results on the EMBER dataset.

Since the BODMAS dataset does not exhibit significant drift, we curated an additional variant by limiting the number of malware families in the training data to evaluate model performance under more severe drift. This setting, described

TABLE IV: Performance on BODMAS dataset.

Method		F1	FPR	FNR
Offline ML	RF	96.3±0.30	0.21±0.01	6.69±0.55
	XGBoost	<u>99.2±0.00</u>	0.30±0.00	1.23±0.00
	MLP	98.2±0.32	0.64±0.15	2.89±0.69
Self-Training	ARF	97.5±0.00	2.13±0.00	2.28±0.00
	DE++	90.78±1.0	15.1±1.88	1.83±0.69
	Insomnia	97.2±0.28	0.56±0.05	4.81±0.51
	MORSE	98.8±0.12	0.48±0.06	1.73±0.32
Proposed	RF+ADAPT	96.1±0.42	0.22±0.01	7.11±0.75
	XGBoost+ADAPT	99.6±0.02	0.34±0.01	0.61±0.03
	MLP+ADAPT	98.6±0.25	0.41±0.02	2.26±0.50

TABLE V: Performance on EMBER dataset.

Method		F1	FPR	FNR
Offline ML	RF	86.3±0.29	3.47±0.02	21.7±0.45
	XGBoost	<u>92.3±0.00</u>	3.58±0.00	11.4±0.00
	MLP	88.1±0.28	5.66±0.50	17.1±0.39
Self-Training	ARF	69.7±0.00	91.8±0.00	1.78±0.00
	DE++	76.9±0.82	24.9±0.73	22.8±1.21
	Insomnia	87.1±0.35	6.06±0.13	18.5±0.66
	MORSE	89.8±0.22	6.34±0.16	13.7±0.36
Proposed	RF+ADAPT	86.2±0.26	3.56±0.03	21.7±0.42
	XGBoost+ADAPT	93.5±0.05	4.45±0.07	8.70±0.11
	MLP+ADAPT	89.1±0.37	5.01±0.18	16.0±0.73

in Appendix F, demonstrates that ADAPT exhibits greater resilience to distributional shifts.

b) **EMBER dataset:** For the EMBER dataset, the baseline XGBoost model outperforms all self-training methods. Our method further improves upon the XGBoost baseline by 1.2%. Among the baseline self-training models, DE++ and ARF perform substantially worse than the baseline models, suggesting they are more susceptible to self-poisoning and highly sensitive to threshold settings on these datasets.

D. PDF Dataset

Table VI presents the results on the PDF malware dataset. Interestingly, Random Forest outperforms both XGBoost and MLP on this dataset, suggesting that more complex models may be prone to overfitting. Nonetheless, our proposed method, ADAPT, improves the F1-score by 1.1%, primarily due to a reduction in the False Negative Rate (FNR). This result again highlights the effectiveness of our model-agnostic approach, which can enhance performance across different classifiers.

E. Effectiveness of ADAPT Across Models

We designed ADAPT as a model-agnostic adaptation strategy and demonstrated its ability to improve performance across different models. Our goal was to show that ADAPT enhances baseline models (RF, XGBoost, MLP) in the presence of concept drift. While different models may be preferable in various deployment settings, XGBoost+ADAPT emerges as a strong default choice, achieving the highest F1-score on three out of five datasets.

TABLE VI: Performance on PDF malware dataset.

	Method	F1	FPR	FNR
Offline ML	RF	98.0 ± 0.87	0.07 ± 0.00	3.31 ± 1.57
	XGBoost	97.9 ± 0.95	0.14 ± 0.04	3.17 ± 1.50
	MLP	97.4 ± 0.17	0.11 ± 0.01	4.26 ± 0.30
Self-Training	ARF	29.7 ± 0.00	0.01 ± 0.00	80.0 ± 0.00
	DE++	60.8 ± 10.5	19.3 ± 6.70	0.28 ± 0.06
	Insomnia	88.2 ± 7.41	0.09 ± 0.02	15.4 ± 8.87
	MORSE	97.4 ± 0.13	0.12 ± 0.01	4.16 ± 0.22
Proposed	RF+ADAPT	99.1 ± 0.11	0.09 ± 0.00	1.26 ± 0.20
	XGBoost+ADAPT	98.6 ± 0.36	0.10 ± 0.00	2.03 ± 0.67
	MLP+ADAPT	97.2 ± 0.12	0.09 ± 0.01	4.73 ± 0.24

TABLE VII: Difference between False Positive Rate (FPR) and False Negative Rate (FNR) across different models and datasets. Positive values indicate a reduction in error, while negative values indicate an increase in error using the proposed ADAPT algorithm.

Model	Metric	Drebin	APIGraph	BODMAS	EMBER	PDF
RF	Δ FPR	-0.07	0.00	-0.01	-0.09	-0.02
	Δ FNR	14.4	20.9	-0.42	0.00	2.05
	Δ FNR	9.00	20.5	0.62	2.70	1.14
XGBoost	Δ FPR	0.42	-1.30	0.06	-0.87	0.04
	Δ FNR	9.00	20.5	0.62	2.70	1.14
	Δ FNR	10.7	20.5	0.63	1.10	-0.47

Although MLP+ADAPT achieves the highest performance over the full six-year test period on the APIGraph dataset, XGBoost+ADAPT (83.7% F1) outperforms both MLP+ADAPT (82.7% F1) and MORSE (80.5% F1) in the first year of test data, a timeframe that more realistically represents practical deployment scenarios for unlabeled adaptation. This highlights that while ADAPT is model-agnostic, its strong synergy with XGBoost enhances its versatility as a broadly applicable solution. A statistical analysis of ADAPT, provided in Appendix E, further substantiates this finding.

F. Error Analysis

Table VII summarizes the changes in False Positive Rate (FPR) and False Negative Rate (FNR) between baseline models and those trained with ADAPT. Across datasets, F1-score improvements are mainly due to reduced FNR, except for Random Forest on BODMAS and MLP on PDF. This suggests that ADAPT enables the model to better learn from uncertain malware samples, improving its ability to correctly classify similar cases upon retraining. In most scenarios, FPR is maintained or reduced alongside FNR, though exceptions exist—e.g., XGBoost on APIGraph, which shows decreased FNR but increased FPR. Neural networks generally outperform other models in reducing FPR. We further examine this in the context of pseudo-labeling errors on APIGraph.

Figure 9 shows the pseudo-labeling errors introduced during the test months for the three ADAPT-trained models on the APIGraph dataset. Here, $err_{p,b}$ denotes the fraction of malware samples incorrectly pseudo-labeled as benign, and $err_{p,m}$ denotes benign samples mislabeled as malware. Across all models, $err_{p,b}$ is significantly lower than $err_{p,m}$, indicating

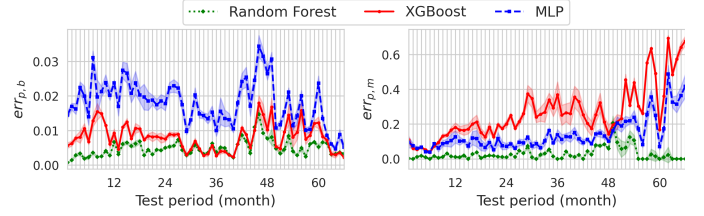


Fig. 9: Pseudo-labeling errors during the test months on the APIGraph dataset. (Left): Fraction of samples incorrectly pseudo-labeled as benign. (Right): Fraction of samples incorrectly pseudo-labeled as malware.

TABLE VIII: Performance metrics (F1, FPR, FNR) for RF, XGBoost, and MLP with various components removed on the first six months of the APIGraph test set.

Component Removed	RF			XGBoost			MLP		
	F1	FPR	FNR	F1	FPR	FNR	F1	FPR	FNR
None	83.6	0.25	26.6	86.7	1.06	16.0	85.2	0.66	21.4
Adaptive Th.	80.8	0.17	31.2	86.4	1.00	16.8	81.2	0.50	25.1
Augmentation	82.3	0.21	28.8	85.6	1.11	17.5	84.8	0.75	21.4
Mixup	83.5	0.25	26.7	86.5	0.97	16.9	81.5	0.54	27.8

that benign pseudo-labels are generally more accurate. This can be attributed to the higher thresholds for selecting benign samples: the optimal values of τ_b for Random Forest, XGBoost, and MLP are 0.96, 0.97, and 0.98, respectively. These high thresholds ensure that only samples with high benign confidence are selected, which helps prevent FNR degradation. This strategy is essential, as evasive malware may exhibit features similar to benign samples. Lowering the threshold could result in mislabeling such malware as benign, negatively impacting FNR.

Conversely, $err_{p,m}$ is notably higher due to the lower threshold τ_m used for pseudo-labeling malware samples—0.67, 0.70, and 0.63 for Random Forest, XGBoost, and MLP, respectively. These lower thresholds increase the likelihood of mislabeling benign samples as malware, a problem that intensifies over time, especially beyond four years. This explains the rise in FPR for XGBoost. Despite also introducing many noisy pseudo-labels, the MLP model reduces FPR compared to its baseline, likely due to the inherent robustness of neural networks to label noise in semi-supervised learning with data augmentation [69]. From a threat modeling perspective, using a lower threshold for malware selection is reasonable—benign apps lack the motivation to evade detection, so lower-confidence malware predictions still provide valuable drifted samples for retraining. While this increases the risk of labeling errors, it is essential for maintaining adaptability against evolving threats.

G. Ablation Study

We conduct an ablation study by removing different components of ADAPT on the APIGraph dataset, as shown in Table VIII for the first six months of test data. In this experiment, we replace the class-specific adaptive thresholding scheme with a fixed threshold of τ_b . We observe that each component

TABLE IX: Performance on Drebin and APIGraph with active learning (AL) with 50 monthly annotation budget.

Dataset	Method	F1	FPR	FNR
Drebin	XGBoost	62.5±1.95	0.57±0.04	47.7±1.85
	XGBoost + AL	<u>81.3±0.00</u>	0.14±0.00	29.0±0.00
	HCC	68.5±3.38	0.57±0.05	40.3±4.37
	XGBoost + ADAPT + AL	81.7±0.28	0.16±0.01	27.8±0.44
APIGraph	XGBoost	79.2±0.43	0.98±0.06	24.2±1.20
	XGBoost + AL	<u>88.7±0.00</u>	0.36±0.00	15.8±0.00
	HCC	86.7±0.15	0.56±0.03	17.2±0.36
	XGBoost + ADAPT + AL	89.4±0.17	0.79±0.02	9.55±0.18

contributes to the overall improvement in F1-score and FNR, albeit varying degrees across different models. While replacing adaptive thresholding reduces the FPR marginally due to the higher threshold, as discussed in Section VII-F, it leads to a significant increase in the FNR, as drifted malware samples are not included in the retraining phase.

VIII. COMPATIBILITY WITH ACTIVE LEARNING

While ADAPT demonstrates significant improvements and can delay the onset of concept drift, at some point, labeled data may become necessary to handle drift effectively [38]. Active learning has proven to be one of the most effective approaches for addressing this issue in malware detection [23], [37]. Although the combination of semi-supervised and active learning has been explored in low-data scenarios [30], [65], its application to malware detection under concept drift remains largely unexplored. We explore this combination for the two Android malware detection datasets.

We follow the approach from [65], where the samples with the highest uncertainty (i.e., the lowest predicted probability) are selected for human annotation using active learning, while high-quality pseudo-labels are selected using ADAPT at every retraining step. We incorporate active learning into ADAPT with a slight modification in Algorithm 1. We adopt the same active learning setup as in [2], [23]. Specifically, we first sample the k most uncertain samples for human annotation for each test month, where k represents the monthly annotation budget. These samples are then added to the labeled training dataset D_l , which increases in size by k each month. Following this, we perform Step 1 in Algorithm 1 to select pseudo-labeled samples using adaptive thresholding. However, we exclude the samples that have already been annotated through active learning, as we already have ground truth labels for them. We then continue with the rest of the algorithm and retrain the model. We perform a random hyperparameter search with 100 iterations, similar to [2].

Table IX presents the results with a monthly annotation budget of 50 on the Android datasets. For the XGBoost baseline model, we randomly select the same number of annotated samples per month to ensure consistency with the active learning methods following [11]. We report active learning results based on uncertainty sampling, using XGBoost and the Hierarchical Contrastive Learning Classifier (HCC) introduced in [23]. HCC, the state-of-the-art method for active learning

with neural networks, leverages contrastive learning with a hierarchical loss function to distinguish between samples from different malware families in the embedding space.

From Table IX, we observe that active learning improves performance over random selection for the XGBoost model. Furthermore, ADAPT enhances this performance by leveraging the remaining unlabeled data. Specifically, we observe a 0.4% increase in F1-score for the Drebin dataset and a 0.7% improvement for APIGraph. While these gains are relatively modest, they indicate that ADAPT can effectively benefit from active learning. Although our current approach involves a straightforward integration with active learning, exploring more sophisticated applications remains an avenue for future work.

IX. EXTENSION TO MULTICLASS CLASSIFICATION

While we designed ADAPT primarily for binary malware detection, this section explores its applicability to a multiclass classification task. Specifically, we consider Windows malware family classification and construct two datasets from the BODMAS and EMBER datasets.

Datasets. We follow the same temporal split as in the binary classification task for training, validation, and test splits in both datasets. We select the top 10 most frequent malware families for each dataset in the training split and include the benign class, resulting in an 11-class classification task. We perform a hyperparameter search on the BODMAS dataset using 100 iterations per model and apply the selected hyperparameters directly to the EMBER dataset without further tuning. Appendix C provides additional details on these datasets.

Algorithm Adjustments. In the binary detection setting, we use separate threshold parameters, τ_b for benign samples and τ_m for malware samples, updated dynamically based on model predictions on unlabeled data using the adaptation parameter λ . While λ is shared across all classes, introducing separate thresholds for each malware family in the multiclass setting would significantly increase the number of parameters, complicating hyperparameter tuning. To mitigate this, we share τ_m across all malware classes, keeping the number of hyperparameters the same as in the binary setting (five), regardless of the number of malware families. Appendix C explores a scenario without a benign class, where only malware families are classified. Apart from this threshold adjustment, the rest of the algorithm, including augmentation and mixup, remains unchanged.

Results. We report the macro F1-score, precision, and recall in Table X for the XGBoost baseline, other self-training methods, and XGBoost+ADAPT on the two datasets. While ADAPT improves over the baseline on both datasets, other self-training methods perform worse than the XGBoost baseline. This effect is particularly pronounced in the EMBER dataset, which is more challenging and where we do not perform additional hyperparameter tuning. Notably, ADAPT improves the average F1-score over XGBoost by 2.8%, whereas other self-training methods perform significantly worse than the baseline, sug-

TABLE X: Performance on multiclass classification (11-class) on BODMAS and EMBER datasets.

Dataset	Method	F1	Precision	Recall
BODMAS	XGBoost	71.0±0.00	75.7±0.00	72.5±0.00
	ARF	57.4±0.00	59.1±0.00	64.1±0.00
	MORSE	68.1±2.21	67.8±4.68	73.1±0.78
	Insomnia	70.1±1.21	71.6±0.99	73.6±1.70
	XGBoost+ADAPT	71.4±0.65	75.6±1.27	72.6±0.61
EMBER	XGBoost	62.4±0.00	70.6±0.00	68.7±0.00
	ARF	11.0±0.00	11.8±0.00	17.7±0.00
	MORSE	58.4±1.49	68.4±1.11	64.5±1.02
	Insomnia	52.7±0.78	66.4±0.28	57.7±0.67
	XGBoost+ADAPT	65.2±0.65	70.3±0.94	71.4±0.59

TABLE XI: Model performance as unknown malware from new families is introduced during testing.

Metric	Additional new families		
	5	10	20
Evasion success rate (%)	9.83	7.10	6.59
AUC	0.706	0.713	0.713

gesting that ADAPT is more robust to hyperparameter values compared to other methods on EMBER feature.

Unknown Family Detection. To evaluate the open-set performance of the multi-class malware classifier, we conducted a monthly analysis with varying levels of novelty in the unknown samples. For each month, we selected the top- k most frequent unseen malware families ($k \in \{5, 10, 20\}$) and computed two key metrics: the *evasion success rate*, defined as the fraction of unknown samples misclassified as benign, and the *AUC*, which reflects the model’s ability to separate known from unknown samples based on confidence scores. This AUC metric aligns with out-of-distribution (OOD) detection [71], where, ideally, lower confidence is assigned to unseen classes. Table XI presents the average results on the EMBER dataset using the XGBoost+ADAPT model, highlighting its tendency to misclassify unknown malware as known malicious classes.

Active Learning. We conduct additional experiments using an annotation budget of 50 samples per month for active learning with the XGBoost model. Table XII presents the results for random sample selection and active learning with the 50 most uncertain samples. Additionally, applying ADAPT with active learning improves performance over the random baseline by 3% on the BODMAS dataset and 2.6% on the EMBER dataset.

X. LIMITATIONS & FUTURE WORK

Evasion and Poisoning Attacks. The effectiveness of our approach may be compromised by adversarial samples designed to evade malware detection classifiers [34]. While we do not explicitly address adversarial examples, integrating adversarial robustness techniques [14] could enhance resilience. Additionally, poisoning attacks can impact continual learning updates [61]; if an adversary crafts a misclassified sample with high confidence, it may increase false negatives or false positives through pseudo-labeling errors. However, semi-supervised learning methods may offer some resistance to label

TABLE XII: Performance on multiclass classification on BODMAS and EMBER datasets with active learning.

Dataset	Method	F1	Precision	Recall
BODMAS	XGBoost	73.1±0.37	77.6±0.29	74.7±0.61
	XGBoost + AL	73.9±0.00	79.7±0.00	75.4±0.00
	XGBoost+ADAPT + AL	76.1±0.68	79.4±1.10	77.8±0.59
EMBER	XGBoost	78.0±0.51	80.6±0.35	82.4±0.54
	XGBoost + AL	78.2±0.00	80.5±0.00	82.6±0.00
	XGBoost+ADAPT + AL	80.6±1.00	81.8±1.10	84.5±0.68

noise [69]. We leave the exploration of adversarial robustness in this context as future work.

Computational Efficiency. ADAPT introduces no additional latency during deployment, as its inference time remains identical to that of the baseline model. However, the training time increases linearly due to data augmentation and mixup strategies. We provide a detailed analysis of the computational overhead in Appendix I.

Limitations in Features. Our experiments rely on static analysis features, which may not be sufficient for effectively handling concept drift [28]. Incorporating dynamic features, or a combination of static and dynamic features, could potentially improve the model’s ability to adapt to concept drift. Its effectiveness with dynamic or hybrid features can be explored in future studies.

Catastrophic forgetting. Catastrophic forgetting refers to the tendency of a learned model to lose previously acquired knowledge when trained on new data—a challenge particularly relevant in malware detection [53]. We analyze its impact on the Android malware detection datasets in Appendix H. While our approach does not directly address catastrophic forgetting, future work could jointly integrate mechanisms to handle concept drift and mitigate forgetting. One promising direction is using replay-based methods from continual learning [54]. In our context, this could involve maintaining a replay buffer of class-balanced, confidently pseudo-labeled samples from intermediate time steps, which can be reused during subsequent model fine-tuning.

Applicability to Other Security Domains. Future work could explore extending ADAPT to other security domains, such as intrusion and phishing detection, where concept drift occurs frequently. While effective data augmentation may require domain-specific customization, other key components of ADAPT, such as adaptive thresholding and mixup regularization, remain domain-independent.

XI. CONCLUSION

We propose a pseudo-labeling-based approach to mitigate concept drift in malware detection. Our model-agnostic method demonstrates effectiveness across five different datasets, each with varying degrees of distributional shift. Through these experiments, we show how our approach addresses limitations found in prior pseudo-labeling methods applied to malware detection. Additionally, our method is compatible with active learning, offering a pathway for further improvement in handling concept drift.

REFERENCES

- [1] Hojjat Aghakhani, Fabio Gritti, Francesco Mecca, Martina Lindorfer, Stefano Ortolani, Davide Balzarotti, Giovanni Vigna, and Christopher Kruegel. When malware is packin'heat; limits of machine learning classifiers based on static analysis features. In *Network and Distributed Systems Security (NDSS) Symposium 2020*, 2020.
- [2] Md Tanvirul Alam, Dipkamal Bhushal, and Nidhi Rastogi. Revisiting static feature-based android malware detection. *arXiv preprint arXiv:2409.07397*, 2024.
- [3] Md Tanvirul Alam, Romy Fieblinger, Ashim Mahara, and Nidhi Rastogi. Morph: Towards automated concept drift adaptation for malware detection. *arXiv preprint arXiv:2401.12790*, 2024.
- [4] Mohammed S Alam and Son T Vuong. Random forest classification for detecting android malware. In *2013 IEEE international conference on green computing and communications and IEEE Internet of Things and IEEE cyber, physical and social computing*, pages 663–669. IEEE, 2013.
- [5] Kevin Allix, Tegawendé F Bissyandé, Jacques Klein, and Yves Le Traon. Are your training datasets yet relevant? an investigation into the importance of timeline in machine learning-based malware detection. In *International Symposium on Engineering Secure Software and Systems*, pages 51–67. Springer, 2015.
- [6] David Alvarez-Melis and Nicolo Fusi. Geometric dataset distances via optimal transport. *Advances in Neural Information Processing Systems*, 33:21428–21439, 2020.
- [7] Massih-Reza Amini, Vasilii Feofanov, Loic Pauletto, Lies Hadjadj, Emilie Devijver, and Yury Maximov. Self-training: A survey. *arXiv preprint arXiv:2202.12040*, 2022.
- [8] H. S. Anderson and P. Roth. EMBER: An Open Dataset for Training Static PE Malware Machine Learning Models. *ArXiv e-prints*, April 2018.
- [9] Hyrum S Anderson, Anant Kharkar, Bobby Filar, David Evans, and Phil Roth. Learning to evade static pe machine learning malware models via reinforcement learning. *arXiv preprint arXiv:1801.08917*, 2018.
- [10] Giuseppina Andresini, Feargus Pendlebury, Fabio Pierazzi, Corrado Loglisci, Annalisa Appice, and Lorenzo Cavallaro. Insomnia: towards concept-drift robustness in network intrusion detection. In *Proceedings of the 14th ACM workshop on artificial intelligence and security*, pages 111–122, 2021.
- [11] Giovanni Apruzzese, Pavel Laskov, and Aliya Tastemirova. Sok: The impact of unlabelled data in cyberthreat detection. In *2022 IEEE 7th European Symposium on Security and Privacy (EuroS&P)*, pages 20–42. IEEE, 2022.
- [12] Eric Arazo, Diego Ortego, Paul Albert, Noel E O'Connor, and Kevin McGuinness. Pseudo-labeling and confirmation bias in deep semi-supervised learning. In *2020 International joint conference on neural networks (IJCNN)*, pages 1–8. IEEE, 2020.
- [13] Daniel Arp, Michael Spreitzerbarth, Malte Hubner, Hugo Gascon, Konrad Rieck, and CERT Siemens. Drebin: Effective and explainable detection of android malware in your pocket. In *NDSS*, volume 14, pages 23–26, 2014.
- [14] Tao Bai, Jinqi Luo, Jun Zhao, Bihan Wen, and Qian Wang. Recent advances in adversarial training for adversarial robustness. *arXiv preprint arXiv:2102.01356*, 2021.
- [15] Federico Barbero, Feargus Pendlebury, Fabio Pierazzi, and Lorenzo Cavallaro. Transcending transcend: Revisiting malware classification in the presence of concept drift. In *2022 IEEE Symposium on Security and Privacy (SP)*, pages 805–823. IEEE, 2022.
- [16] James Bergstra and Yoshua Bengio. Random search for hyper-parameter optimization. *Journal of machine learning research*, 13(2), 2012.
- [17] David Berthelot, Nicholas Carlini, Ian Goodfellow, Nicolas Papernot, Avital Oliver, and Colin A Raffel. Mixmatch: A holistic approach to semi-supervised learning. *Advances in neural information processing systems*, 32, 2019.
- [18] Christopher M Bishop and Nasser M Nasrabadi. *Pattern recognition and machine learning*, volume 4. Springer, 2006.
- [19] Tobias Braun, Irdin Pekaric, and Giovanni Apruzzese. Understanding the process of data labeling in cybersecurity. In *Proceedings of the 39th ACM/SIGAPP Symposium on Applied Computing*, pages 1596–1605, 2024.
- [20] Leo Breiman. Random forests. *Machine learning*, 45:5–32, 2001.
- [21] J Paul Brooks. Support vector machines with the ramp loss and the hard margin loss. *Operations research*, 59(2):467–479, 2011.
- [22] Tianqi Chen and Carlos Guestrin. Xgboost: A scalable tree boosting system. In *Proceedings of the 22nd acm sigkdd international conference on knowledge discovery and data mining*, pages 785–794, 2016.
- [23] Yizheng Chen, Zhoujie Ding, and David A. Wagner. Continuous learning for android malware detection. In Joseph A. Calandrina and Carmela Troncoso, editors, *32nd USENIX Security Symposium, USENIX Security 2023, Anaheim, CA, USA, August 9-11, 2023*, pages 1127–1144. USENIX Association, 2023.
- [24] Yizheng Chen, Shiqi Wang, Dongdong She, and Suman Jana. On training robust pdf malware classifiers. In *Proceedings of the 29th USENIX Conference on Security Symposium*, pages 2343–2360, 2020.
- [25] Zhi Chen, Zhenning Zhang, Zeliang Kan, Limin Yang, Jacopo Cortelazzi, Feargus Pendlebury, Fabio Pierazzi, Lorenzo Cavallaro, and Gang Wang. Is it overkill? analyzing feature-space concept drift in malware detectors. In *2023 IEEE Security and Privacy Workshops (SPW)*, pages 21–28. IEEE, 2023.
- [26] Theo Chow, Zeliang Kan, Lorenz Linhardt, Lorenzo Cavallaro, Daniel Arp, and Fabio Pierazzi. Drift forensics of malware classifiers. In *Proceedings of the 16th ACM Workshop on Artificial Intelligence and Security*, pages 197–207, 2023.
- [27] Ekin D Cubuk, Barret Zoph, Jonathon Shlens, and Quoc V Le. Randaugment: Practical automated data augmentation with a reduced search space. In *Proceedings of the IEEE/CVF conference on computer vision and pattern recognition workshops*, pages 702–703, 2020.
- [28] Savino Dambra, Yufei Han, Simone Aonzo, Platon Kotzias, Antonino Vitale, Juan Caballero, Davide Balzarotti, and Leyla Bilge. Decoding the secrets of machine learning in malware classification: A deep dive into datasets, feature extraction, and model performance. In *Proceedings of the 2023 ACM SIGSAC Conference on Computer and Communications Security*, pages 60–74, 2023.
- [29] Cuiying Gao, Gaozhun Huang, Heng Li, Bang Wu, Yueming Wu, and Wei Yuan. A comprehensive study of learning-based android malware detectors under challenging environments. In *Proceedings of the 46th IEEE/ACM International Conference on Software Engineering*, pages 1–13, 2024.
- [30] Mingfei Gao, Zizhao Zhang, Guo Yu, Sercan Ö Arık, Larry S Davis, and Tomas Pfister. Consistency-based semi-supervised active learning: Towards minimizing labeling cost. In *Computer vision—ECCV 2020: 16th European conference, glasgow, UK, August 23–28, 2020, proceedings, part x 16*, pages 510–526. Springer, 2020.
- [31] Josh Gardner, Zoran Popovic, and Ludwig Schmidt. Benchmarking distribution shift in tabular data with tableshift. *Advances in Neural Information Processing Systems*, 36, 2024.
- [32] Heitor M Gomes, Albert Bifet, Jesse Read, Jean Paul Barddal, Fabrício Enembreck, Bernhard Pfahringer, Geoff Holmes, and Talel Abdesslem. Adaptive random forests for evolving data stream classification. *Machine Learning*, 106:1469–1495, 2017.
- [33] Léo Grinsztajn, Edouard Oyallon, and Gaël Varoquaux. Why do tree-based models still outperform deep learning on typical tabular data? *Advances in neural information processing systems*, 35:507–520, 2022.
- [34] Kathrin Grosse, Nicolas Papernot, Praveen Manoharan, Michael Backes, and Patrick McDaniel. Adversarial perturbations against deep neural networks for malware classification. *arXiv preprint arXiv:1606.04435*, 2016.
- [35] Martin Heusel, Hubert Ramsauer, Thomas Unterthiner, Bernhard Nessler, and Sepp Hochreiter. Gans trained by a two time-scale update rule converge to a local nash equilibrium. *Advances in neural information processing systems*, 30, 2017.
- [36] Maryam Issakhani, Princy Victor, Ali Tekeoglu, and Arash Habibi Lashkari. Pdf malware detection based on stacking learning. In *ICISSP*, pages 562–570, 2022.
- [37] Roberto Jordaney, Kumar Sharad, Santanu K Dash, Zhi Wang, Davide Papini, Ilia Nouretdinov, and Lorenzo Cavallaro. Transcend: Detecting concept drift in malware classification models. In *26th USENIX security symposium (USENIX security 17)*, pages 625–642, 2017.
- [38] Zeliang Kan, Feargus Pendlebury, Fabio Pierazzi, and Lorenzo Cavallaro. Investigating labelless drift adaptation for malware detection. In *Proceedings of the 14th ACM Workshop on Artificial Intelligence and Security*, pages 123–134, 2021.
- [39] Ananya Kumar, Tengyu Ma, and Percy Liang. Understanding self-training for gradual domain adaptation. In *International Conference on Machine Learning*, pages 5468–5479. PMLR, 2020.
- [40] Dong-Hyun Lee et al. Pseudo-label: The simple and efficient semi-supervised learning method for deep neural networks. In *Workshop*

- on challenges in representation learning, *ICML*, volume 3, page 896. Atlanta, 2013.
- [41] Chi-Heng Lin, Chiraag Kaushik, Eva L Dyer, and Vidya Muthukumar. The good, the bad and the ugly sides of data augmentation: An implicit spectral regularization perspective. *Journal of Machine Learning Research*, 25(91):1–85, 2024.
 - [42] Martina Lindorfer, Matthias Neugschwandtner, and Christian Platzter. Marvin: Efficient and comprehensive mobile app classification through static and dynamic analysis. In *2015 IEEE 39th annual computer software and applications conference*, volume 2, pages 422–433. IEEE, 2015.
 - [43] Jie Lu, Anjin Liu, Fan Dong, Feng Gu, Joao Gama, and Guangquan Zhang. Learning under concept drift: A review. *IEEE transactions on knowledge and data engineering*, 31(12):2346–2363, 2018.
 - [44] Samaneh MahdaviFar, Andi Fitriah Abdul Kadir, Rasool Fatemi, Dima Alhadidi, and Ali A. Ghorbani. Dynamic android malware category classification using semi-supervised deep learning. In *Proc. IEEE DASC/PiCom/CBDCom/CyberSciTech*, pages 515–522, 2020.
 - [45] Brad Miller, Alex Kantchelian, Michael Carl Tschantz, Sadia Afroz, Rekha Bachwani, Riyaz Faizullahoy, Ling Huang, Vaishaal Shankar, Tony Wu, George Yiu, et al. Reviewer integration and performance measurement for malware detection. In *Detection of Intrusions and Malware, and Vulnerability Assessment: 13th International Conference, DIMVA 2016, San Sebastián, Spain, July 7-8, 2016, Proceedings 13*, pages 122–141. Springer, 2016.
 - [46] Annamalai Narayanan, Mahinthan Chandramohan, Lihui Chen, and Yang Liu. Context-aware, adaptive, and scalable android malware detection through online learning. *IEEE Transactions on Emerging Topics in Computational Intelligence*, 1(3):157–175, 2017.
 - [47] Nir Nissim, Robert Moskovitch, Lior Rokach, and Yuval Elovici. Novel active learning methods for enhanced pc malware detection in windows os. *Expert Systems with Applications*, 41(13):5843–5857, 2014.
 - [48] Fakhroddin Noorbehbahani and Mohammad Saberi. Ransomware detection with semi-supervised learning. In *2020 10th International Conference on Computer and Knowledge Engineering (ICCKE)*, pages 024–029. IEEE, 2020.
 - [49] Lucky Onwuzurike, Enrico Mariconti, Panagiotis Andriotis, Emiliano De Cristofaro, Gordon J. Ross, and Gianluca Stringhini. Mamadroid: Detecting android malware by building markov chains of behavioral models (extended version). *ACM Trans. Priv. Secur.*, 22(2):14:1–14:34, 2019.
 - [50] Feargus Pendlebury, Fabio Pierazzi, Roberto Jordaney, Johannes Kinder, Lorenzo Cavallaro, et al. Tesseract: Eliminating experimental bias in malware classification across space and time. In *Proceedings of the 28th USENIX Security Symposium*, pages 729–746. USENIX Association, 2019.
 - [51] Joaquin Quiñero-Candela, Masashi Sugiyama, Anton Schwaighofer, and Neil D Lawrence. *Dataset shift in machine learning*. Mit Press, 2022.
 - [52] Dima Rabadi and Sin G Teo. Advanced windows methods on malware detection and classification. In *Proceedings of the 36th Annual Computer Security Applications Conference*, pages 54–68, 2020.
 - [53] Mohammad Saidur Rahman, Scott Coull, and Matthew Wright. On the limitations of continual learning for malware classification. In *Conference on Lifelong Learning Agents*, pages 564–582. PMLR, 2022.
 - [54] David Rolnick, Arun Ahuja, Jonathan Schwarz, Timothy Lillicrap, and Gregory Wayne. Experience replay for continual learning. *Advances in neural information processing systems*, 32, 2019.
 - [55] David E Rumelhart, Geoffrey E Hinton, and Ronald J Williams. Learning representations by back-propagating errors. *nature*, 323(6088):533–536, 1986.
 - [56] Igor Santos, Javier Nieves, and Pablo G Bringas. Semi-supervised learning for unknown malware detection. In *International Symposium on Distributed Computing and Artificial Intelligence*, pages 415–422. Springer, 2011.
 - [57] Weiwei Shi, Yihong Gong, Chris Ding, Zhiheng MaXiaoyu Tao, and Nanning Zheng. Transductive semi-supervised deep learning using min-max features. In *Proceedings of the European Conference on Computer Vision (ECCV)*, pages 299–315, 2018.
 - [58] Rami Sihwail, Khairuddin Omar, and KA Zainol Ariffin. A survey on malware analysis techniques: Static, dynamic, hybrid and memory analysis. *Int. J. Adv. Sci. Eng. Inf. Technol.*, 8(4-2):1662–1671, 2018.
 - [59] Kihyuk Sohn, David Berthelot, Nicholas Carlini, Zizhao Zhang, Han Zhang, Colin A Raffel, Ekin Dogus Cubuk, Alexey Kurakin, and Chun-Liang Li. Fixmatch: Simplifying semi-supervised learning with consistency and confidence. *Advances in neural information processing systems*, 33:596–608, 2020.
 - [60] Nedim Šrđić and Pavel Laskov. Hidost: a static machine-learning-based detector of malicious files. *EURASIP Journal on Information Security*, 2016:1–20, 2016.
 - [61] Rahim Taheri, Reza Javidan, Mohammad Shojafar, Zahra Pooranian, Ali Miri, and Mauro Conti. On defending against label flipping attacks on malware detection systems. *Neural Computing and Applications*, 32:14781–14800, 2020.
 - [62] Kimberly Tam, Ali Feizollah, Nor Badrul Anuar, Rosli Salleh, and Lorenzo Cavallaro. The evolution of android malware and android analysis techniques. *ACM Computing Surveys (CSUR)*, 49(4):1–41, 2017.
 - [63] Romain Thomas. Lief - library to instrument executable formats. <https://lief.quarkslab.com/>, apr 2017.
 - [64] Sunil Thulasidasan, Gopinath Chennupati, Jeff A Birmes, Tanmoy Bhat-tacharya, and Sarah Michalak. On mixup training: Improved calibration and predictive uncertainty for deep neural networks. *Advances in neural information processing systems*, 32, 2019.
 - [65] Katrin Tomanek and Udo Hahn. Semi-supervised active learning for sequence labeling. In *Proceedings of the Joint Conference of the 47th Annual Meeting of the ACL and the 4th International Joint Conference on Natural Language Processing of the AFNLP*, pages 1039–1047, 2009.
 - [66] Cédric Villani et al. *Optimal transport: old and new*, volume 338. Springer, 2008.
 - [67] Yanshuo Wang, Jie Hong, Ali Cheraghian, Shafin Rahman, David Ahmedt-Aristizabal, Lars Petersson, and Mehrtash Harandi. Continual test-time domain adaptation via dynamic sample selection. In *Proceedings of the IEEE/CVF Winter Conference on Applications of Computer Vision*, pages 1701–1710, 2024.
 - [68] Frank Wilcoxon. Individual comparisons by ranking methods. In *Breakthroughs in statistics: Methodology and distribution*, pages 196–202. Springer, 1992.
 - [69] Xian Wu, Wenbo Guo, Jia Yan, Baris Coskun, and Xinyu Xing. From grim reality to practical solution: Malware classification in real-world noise. In *2023 IEEE Symposium on Security and Privacy (SP)*, pages 2602–2619. IEEE Computer Society, 2023.
 - [70] Ke Xu, Yingjiu Li, Robert Deng, Kai Chen, and Jiayun Xu. Droidevolver: Self-evolving android malware detection system. In *2019 IEEE European Symposium on Security and Privacy (EuroS&P)*, pages 47–62. IEEE, 2019.
 - [71] Jingkan Yang, Kaiyang Zhou, Yixuan Li, and Ziwei Liu. Generalized out-of-distribution detection: A survey. *International Journal of Computer Vision*, 132(12):5635–5662, 2024.
 - [72] Limin Yang, Arridhana Ciptadi, Ihar Laziuk, Ali Ahmadzadeh, and Gang Wang. Bodmas: An open dataset for learning based temporal analysis of pe malware. In *2021 IEEE Security and Privacy Workshops (SPW)*, pages 78–84. IEEE, 2021.
 - [73] Limin Yang, Wenbo Guo, Qingying Hao, Arridhana Ciptadi, Ali Ahmadzadeh, Xinyu Xing, and Gang Wang. Cade: Detecting and explaining concept drift samples for security applications. In *USENIX security symposium*, pages 2327–2344, 2021.
 - [74] Hongyi Zhang, Moustapha Cisse, Yann N Dauphin, and David Lopez-Paz. mixup: Beyond empirical risk minimization. *arXiv preprint arXiv:1710.09412*, 2017.
 - [75] Hongyi Zhang, Moustapha Cissé, Yann N. Dauphin, and David Lopez-Paz. mixup: Beyond empirical risk minimization. In *6th International Conference on Learning Representations, ICLR 2018, Vancouver, BC, Canada, April 30 - May 3, 2018, Conference Track Proceedings*. OpenReview.net, 2018.
 - [76] Linjun Zhang, Zhun Deng, Kenji Kawaguchi, Amirata Ghorbani, and James Zou. How does mixup help with robustness and generalization? *arXiv preprint arXiv:2010.04819*, 2020.
 - [77] Xiaohan Zhang, Yuan Zhang, Ming Zhong, Daizong Ding, Yinchi Cao, Yukun Zhang, Mi Zhang, and Min Yang. Enhancing state-of-the-art classifiers with api semantics to detect evolved android malware. In *Proceedings of the 2020 ACM SIGSAC conference on computer and communications security*, pages 757–770, 2020.
 - [78] Yanjie Zhao, Li Li, Haoyu Wang, Haipeng Cai, Tegawendé F Bissyandé, Jacques Klein, and John Grundy. On the impact of sample duplication in machine-learning-based android malware detection. *ACM Transactions on Software Engineering and Methodology (TOSEM)*, 30(3):1–38, 2021.

APPENDIX A CODE AVAILABILITY

Our work leverages publicly available datasets for malware detection, and we provide detailed explanations of how these datasets were adapted for our experimental setup to ensure reproducibility. Code is available at <https://anonymous.4open.science/r/adapt-3006>. Dataset splits, experiment logs, and trained models will be made publicly available upon publication to support further research and replication of our results.

APPENDIX B SELF-TRAINING BASELINES

DroidEvolver [70] and its improved version, DroidEvolver++ (DE++) [38], are notable prior works in Android malware detection using self-training. However, they suffer from performance degradation due to self-poisoning and have not been thoroughly evaluated across different datasets. Beyond these, there is limited research exploring self-training for concept drift adaptation in the context of malware detection. Therefore, besides DE++, we repurpose and implement three well-known self-training algorithms to evaluate alongside our method.

- 1) **Adaptive Random Forest (ARF)** [32]: ARF is an online learning algorithm that adapts to concept drift through an ensemble of decision trees. While ARF typically requires access to ground truth labels for drift detection and model updates, we adapt it by introducing a threshold parameter to select pseudo-labeled samples. This threshold is tuned alongside other tree hyperparameters, enabling ARF to operate in a self-training setting.
- 2) **DroidEvolver++ (DE++)** [38]: DE++ is an enhanced version of DroidEvolver [70], designed to adapt malware detection models to concept drift without continuous ground truth annotations. DE++ employs an ensemble of five linear models—Passive-Aggressive (PA1), Online Gradient Descent (OGD), Adaptive Regularization of Weights (AROW), Regularized Dual Averaging (RDA), and Adaptive Fobos (Ada-Fobos). It uses the ensemble’s predictions to generate pseudo-labels and maintains a fixed-size buffer of recent samples (the app buffer) to monitor model aging. A model is considered “aging” if the proportion of consistent predictions within the buffer falls below a threshold. If this happens, the model is updated using the ensemble’s pseudo-labels.
- 3) **Insomnia** [10]: Insomnia is a concept drift adaptation method for network intrusion detection, employing co-training with a Nearest Centroid (NC) classifier and an MLP. The NC classifier acts as an oracle, providing pseudo-labels to the MLP for its least confident predictions, which are then used to update the MLP. Both the NC classifier and the MLP are updated using pseudo-labeled data. The authors argue that these two classifiers complement each other: the MLP produces uncertainty estimates, while the NC classifier provides pseudo-labels.

TABLE XIII: Statistics of the BODMAS multiclass classification dataset

ID	Family	Train Samples	Validation Samples	Test Samples
0	Benign	3000	3000	6000
1	Wacatac	2337	917	988
2	Upatre	930	1148	1369
3	Mira	586	512	791
4	Small	558	1026	1475
5	Dinwod	405	682	701
6	Wabot	368	748	2405
7	Autorun	363	148	60
8	Musecador	309	717	19
9	Gepys	298	382	255
10	Berbew	284	195	1195

However, we observed that the NC classifier performed poorly on the more complex task of malware detection, so we replaced it with an XGBoost model while retaining the MLP. Additionally, we selected the most confident samples rather than the least confident ones, as the latter led to self-poisoning early in the training phase.

- 4) **MORSE** [69]: MORSE is the state-of-the-art semi-supervised learning method for malware family classification under noisy labels. Since MORSE also employs semi-supervised techniques, we include it as a baseline. It implements the FixMatch [59] algorithm for malware classification, incorporating a novel augmentation strategy that ensures consistency between a weakly augmented pseudo-labeled sample and a strongly augmented version of the same sample.

The first two baseline methods, ARF and DE++, are online methods that process one sample at a time and do not require access to the entire training dataset after the initial training phase. In contrast, the latter two methods—Insomnia and MORSE—use batch training, combining original training data with pseudo-labeled data for model updates. While we primarily assume that training data is available, we also explore scenarios where access to the original training data is restricted, as discussed in Appendix G.

APPENDIX C MULTICLASS CLASSIFICATION

A. Dataset Statistics

Table XIII for the BODMAS dataset and Table XIV for the EMBER dataset present the class-wise statistics for the training, validation, and test sets.

In the BODMAS dataset, we use all available samples from the training split for each malware family and randomly select 1,000 samples per month from the Benign class. The same sampling strategy is applied to the validation and test splits. Notably, some malware families, such as Gepys, are relatively rare in the test set, whereas others, such as Berbew, appear more frequently than in the training data.

Due to the large dataset size, we cap the maximum number of samples per class at 500 for the EMBER training dataset, including the Benign class. This limitation is also enforced for

TABLE XIV: Statics of the EMBER multiclass classification dataset

ID	Family	Train Samples	Test Samples
0	Benign	500	5500
1	InstallMonster	500	3217
2	AdPoshel	500	2647
3	Zusy	500	3783
4	Fareit	500	4662
5	Emotet	500	5386
6	DealPly	500	2227
7	DotDo	500	953
8	StartSurf	500	3819
9	Mira	425	304
10	Tiggre	405	1284

TABLE XV: Performance on multiclass classification (10-class) on BODMAS and EMBER datasets.

Dataset	Method	F1	Precision	Recall
BODMAS	XGBoost	76.8±0.00	82.9±0.00	78.3±0.00
	ARF	63.5±0.00	70.6±0.00	64.0±0.00
	MORSE	75.3±0.86	80.1±1.18	76.4±1.09
	Insomnia	62.2±1.19	69.5±1.47	65.7±1.44
	XGBoost+ADAPT	77.0±1.07	82.2±1.26	77.7±0.99
EMBER	XGBoost	58.7±0.00	67.8±0.00	66.3±0.00
	ARF	10.9±0.00	9.66±0.00	21.1±0.00
	MORSE	53.6±2.23	62.8±1.68	63.1±0.89
	Insomnia	39.6±0.53	58.5±1.31	49.0±0.23
	XGBoost+ADAPT	65.2±1.43	75.1±1.94	70.4±1.35

each month in the test set, ensuring that no class exceeds 500 samples per month. While the training data is approximately balanced across classes, the test data exhibits class imbalance.

B. Experiments Excluding Benign Class

In practice, malware analysis is often a two-step process. The first step involves binary classification to determine whether a sample is benign or malicious. If classified as malware, the next step is to provide additional context by identifying its malware family [53]. We consider this setting for malware family classification here without including the benign class. We remove the benign samples from the BODMAS (Table XIII) and EMBER datasets (Table XIV), resulting in a 10-class classification task.

In this setting, we use a single threshold parameter, τ_m , in ADAPT, shared across all malware families. Aside from this threshold adjustment, the rest of the algorithm remains unchanged between binary and multiclass classification. This modification reduces the number of hyperparameters in ADAPT from five to four.

Table XV presents the results of ADAPT and other self-training approaches across both datasets. ADAPT outperforms the baseline XGBoost methods on both datasets, while other self-training methods perform worse. The improvement is especially notable on the EMBER dataset, where ADAPT achieves a 6.5% increase in the F1-score.

Table XVI presents the results for active learning with a monthly annotation budget of 50 samples. Active learning

TABLE XVI: Performance on multiclass classification (10-class) on BODMAS and EMBER datasets with active learning.

Dataset	Method	F1	Precision	Recall
BODMAS	XGBoost	81.2±0.96	86.2±0.99	81.9±0.96
	XGBoost + AL	83.2±0.00	89.2±0.00	83.6±0.00
	XGBoost+ADAPT + AL	85.5±1.08	90.6±0.37	85.8±1.58
EMBER	XGBoost	76.4±1.22	79.2±1.06	80.6±1.21
	XGBoost + AL	77.1±0.00	79.6±0.00	81.8±0.00
	XGBoost+ADAPT + AL	83.8±0.65	85.0±0.55	87.2±0.40

TABLE XVII: Performance comparison on APIGraph and Drebin datasets using SVM model.

Method	F1	FPR	FNR
APIGraph			
SVM	66.3 ± 0.00	1.41 ± 0.00	39.5 ± 0.00
SVM+ADAPT	73.6 ± 0.13	1.47 ± 0.01	29.3 ± 0.08
Drebin			
SVM	33.8 ± 0.00	0.70 ± 0.00	76.7 ± 0.00
SVM+ADAPT	48.0 ± 0.54	0.84 ± 0.06	61.5 ± 0.60

with uncertainty sampling outperforms the baseline XGBoost model trained with the same annotation budget using random sampling. Additionally, incorporating ADAPT further enhances performance on both datasets. Specifically, integrating ADAPT improves the F1-score by 2.3% on the BODMAS dataset and 6.1% on the EMBER dataset, demonstrating the effectiveness of leveraging unlabeled samples even in the presence of active learning.

APPENDIX D

SUPPORT VECTOR MACHINE(SVM) EXPERIMENTS

We conduct additional experiments using SVM baseline models on two Android datasets, APIGraph and Drebin, using the same hyperparameter selection strategy from Section VI-C. The results, including those with ADAPT, are summarized in Table XVII.

The baseline SVM model performs competitively with the baseline XGBoost model on the APIGraph dataset. However, its performance is significantly lower on the Drebin dataset than the XGBoosr baseline.

Integrating ADAPT with the SVM model proves to be effective, yielding performance improvements over the baseline SVM across both datasets. Notably, ADAPT significantly reduces the false negative rate, improving the F1-score. This effect is particularly pronounced in the Drebin dataset, where we observe an average F1-score increase of 14.2%.

APPENDIX E

STATISTICAL SIGNIFICANCE

Table XVIII presents the Wilcoxon signed-rank test p-values for comparing different machine learning models (Random Forest, MLP, and XGBoost) across multiple malware datasets. The Wilcoxon test [68] is a non-parametric statistical test used to assess whether two paired samples come from the same distribution. In this case, it evaluates whether the adapted

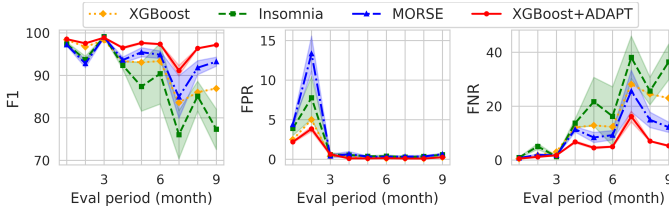


Fig. 10: Performance on the reduced BODMAS dataset (with eight malware families in the training and validation sets) evaluated on validation and test data: F1 score (left), FPR (middle), and FNR (right).

model’s F1-scores significantly differ from the baseline in the test months. Cells are shaded in gray if the p-value is less than 0.05, indicating statistically significant differences. Notably, we observe consistently low p-values for the XGBoost models across all datasets, suggesting a significant effect of adaptation on their performance.

TABLE XVIII: Wilcoxon p-values for different models across datasets. Cells with $p < 0.05$ are shaded.

Dataset	Metric	Random Forest	MLP	XGBoost
p-values				
Drebin	p-value	7.63×10^{-6}	5.34×10^{-5}	1.53×10^{-5}
APIGraph	p-value	1.64×10^{-12}	1.64×10^{-12}	1.23×10^{-10}
BODMAS	p-value	0.6875	0.03125	0.03125
EMBER	p-value	0.7646	0.03223	0.00195
PDF	p-value	0.4375	0.15625	0.03125

Table XIX presents the p-values for active learning using ADAPT with the XGBoost baseline model with 50 randomly annotated samples per month.

TABLE XIX: Wilcoxon p-values for active learning with ADAPT vs baseline XGBoost model (50 annotation budget per month). Cells with $p < 0.05$ are shaded.

Dataset	p-value
Drebin	7.63×10^{-6}
APIGraph	1.64×10^{-12}

APPENDIX F DRIFTED BODMAS DATASET

Since the BODMAS dataset does not exhibit significant drift, we curated an additional dataset to evaluate model performance under more severe drift. For this purpose, we utilized the available malware family information in the dataset. Specifically, we included only the top 8 most frequent malware families from the first three months in the training and validation sets. This corresponds to 5,856 samples or 52.8% of the total malware samples in the training set. We then randomly sampled an equal number of benign samples to include in the training set, as the original dataset has roughly equal distributions of benign and malware samples. The same process was followed for the validation set, comprising the next three months. For the test months, we used the original

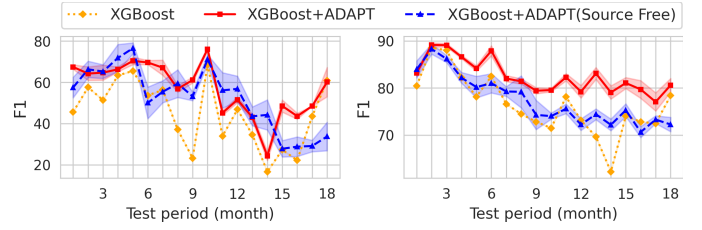


Fig. 11: F1 score on Drebin (left) and APIGraph (right) datasets across the first 18 test months for XGBoost, XGBoost with ADAPT, and XGBoost with ADAPT in a source-free setting (i.e., without access to the training data during retraining).

samples for those months. As a result, the dataset exhibits significant drift starting in the first test month compared to the training and validation data.

We conducted a separate hyperparameter search for this setting and plotted the results of four models in Figure 10. As expected, the baseline XGBoost model deteriorates rapidly starting from month 4 (the first test month) due to a high number of false negatives. In contrast, our proposed method is more resistant to the drift, maintaining relatively high performance, except in month 7, where all models suffer a significant drop in performance.

APPENDIX G SOURCE-FREE ADAPTATION

In some scenarios, access to the original training data may be unavailable after model training due to privacy concerns, proprietary restrictions (for benign applications), storage constraints, or computational limitations [70]. In such cases, the model needs to be updated using only pseudo-labeled data. We explore this possibility for the XGBoost model on the Drebin and APIGraph datasets. The only modification to our proposed Algorithm 1 is in line 7, where $D_m = D_p$, i.e., we only have access to pseudo-labeled data after the initial training period. We perform separate hyperparameter optimization for this setting using the same search space.

Figure 11 shows the results on these datasets, comparing the baseline XGBoost model, the model updated in the semi-supervised learning setup with ADAPT, and the source-free adaptation. For the APIGraph dataset, we plot results for the first 18 months of the test set, as performance deteriorates in the long run (with an overall average F1 score of 61.24%). However, the method shows noticeable benefits within this shorter time frame, even in the source-free setting.

For the Drebin dataset, the source-free adaptation improves the average F1 score by 11.3% over the baseline model in the first year, trailing the semi-supervised variant by only 1.76%. On the APIGraph dataset, it improves over the baseline by 0.82% but trails the semi-supervised baseline by 3.97%. These results suggest that ADAPT can mitigate concept drift to some extent, even when the original training data is unavailable. This makes it a viable option for continual learning settings with storage constraints on the training data, and it can be explored in future research [53].

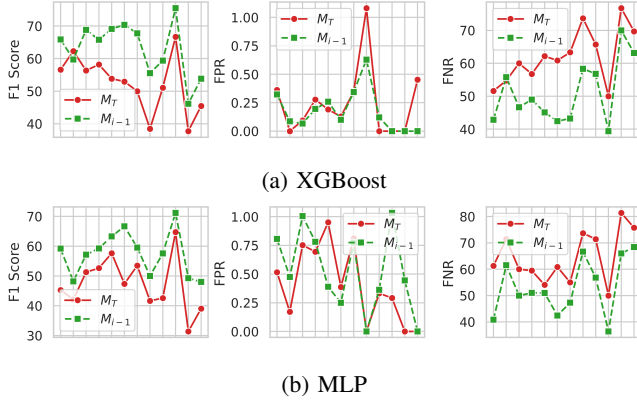


Fig. 12: Impact of catastrophic forgetting on the Drebin dataset for XGBoost and MLP models. The performance is shown over the first 12 months of the test dataset. M_T represents the model trained in the final month, while M_{i-1} denotes the model trained during the preceding month in the retraining process.

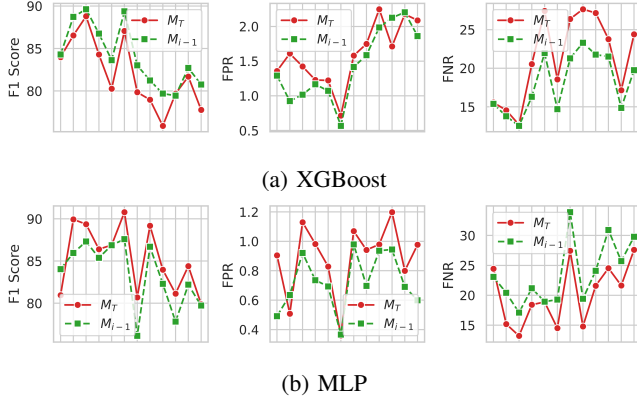


Fig. 13: Impact of catastrophic forgetting on the APIGraph dataset for XGBoost and MLP models.

APPENDIX H CATASTROPHIC FORGETTING

Catastrophic forgetting is a significant concern for any continual learning method, where a model may lose previously learned knowledge when trained on new data [53]. Although addressing catastrophic forgetting is beyond the scope of this work, we assess its impact on the Android malware datasets using XGBoost and MLP.

To assess this, we take the final model trained on the last month (M_T) and evaluate its performance on the first year of test data. We then compare the F1 score, False Positive Rate (FPR), and False Negative Rate (FNR) of the final model against the performance of the model trained during the monthly retraining phase.

The results are presented in Figure 12 for the Drebin dataset and Figure 13 for the APIGraph dataset. Both models exhibit some degree of catastrophic forgetting on the Drebin dataset,

TABLE XX: Training time (in seconds) of different baseline models with ADAPT

Dataset	RF	RF + ADAPT	MLP	MLP + ADAPT	XGBoost	XGBoost + ADAPT
Drebin	38.5	281.0	158.0	712.9	90.3	1378.6
APIGraph	19.5	105.0	32.0	37.0	6.2	17.2
BODMAS	45.9	188.3	242.9	681.6	93.5	301.6
EMBER	111.7	422.1	512.7	1618.5	237.4	668.1
PDF	12.5	57.5	38.1	70.4	6.1	66.0

as the final model’s performance degrades compared to earlier models. In contrast, on the APIGraph dataset, the final MLP model outperforms its earlier versions, indicating no signs of catastrophic forgetting. For the XGBoost model, catastrophic forgetting is primarily driven by an increase in false negatives, whereas for the MLP model, the FNR increases on Drebin but decreases on APIGraph.

APPENDIX I COMPUTATIONAL EFFICIENCY

While ADAPT does not increase inference time, it incurs additional training cost, which increases approximately linearly due to data augmentation and mixup. This overhead is primarily driven by two factors: (1) the time required to generate augmented samples and (2) the additional time needed to train on the expanded dataset, roughly three times larger than the original training set.

The extent of this increase depends on the dataset size, feature dimensionality, and model complexity. Table XX reports the training time overhead introduced by ADAPT across different models and datasets. The most significant increase is observed for the XGBoost model on the Drebin dataset, where the high feature dimensionality (16,978) substantially impacts computation time. For other datasets, training time typically increases by three to five relative to the baseline model.

APPENDIX J DATA AUGMENTATION & CONSISTENCY

We do not explicitly ensure that augmented feature vectors correspond to valid samples, as our augmentation operates in feature space rather than generating samples from a known distribution. Ensuring validity would require modeling complex feature dependencies, which are intractable to the best of our knowledge.

However, we analyze feature correlation structures to assess whether augmentation disrupts dependencies. Specifically, we compute the mean absolute correlation of features in the original dataset to check for strong dependencies. Additionally, we measure the Spearman correlation between the upper triangular elements of the original and augmented correlation matrices to quantify how well feature relationships are preserved.

Table XXI shows feature correlations are generally low across datasets, suggesting weak dependencies. Furthermore, the high Spearman correlation indicates that augmentation does not significantly alter feature relationships. While this

TABLE XXI: Comparison of Feature Correlations Before and After Augmentation

Dataset	Mean $ \rho(X) $	Spearman $(\rho(X), \rho(X_{\text{aug}}))$
APIGraph	0.0238	0.9247
Drebin	0.0269	0.9911
Bodmas	0.0276	0.9491
PDF	0.0857	0.9975

does not guarantee individual sample validity, it provides evidence that the overall statistical structure remains consistent.

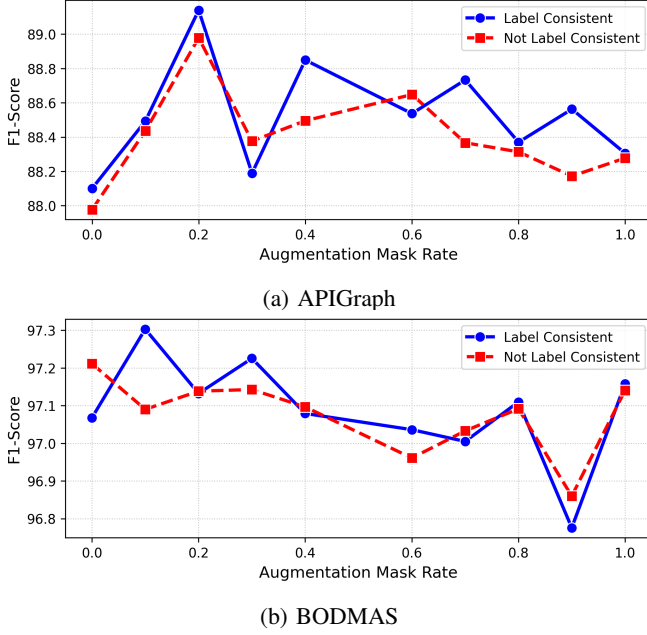


Fig. 14: Validation set performance with and without label consistency as the augmentation mask rate increases.

One way to introduce potentially inconsistent samples is by increasing the strength of augmentation. In our augmentation formulation, this can be achieved by increasing the augmentation mask ratio (m), which controls the fraction of features randomly replaced with features from other samples of the same class.

While we initially set a maximum value of $m = 0.2$ during hyperparameter tuning, we further explore the impact of larger values of m on the APIGraph and BODMAS datasets, which correspond to the Android and Windows feature sets, respectively. Specifically, we vary m from 0.0 to 1.0 while keeping all other hyperparameters fixed at their optimal values for these datasets. Figure 14 presents the F1-scores on the validation set for both datasets. Notably, even for large values of m , performance does not degrade due to augmentation. For instance, when $m = 1.0$, meaning that every feature in a sample is replaced with values drawn from other samples of the same class, the model still outperforms the case where $m = 0.0$ (i.e., no augmentation).

Moreover, we observe that preserving label consistency—by excluding samples where model predictions differ between the

original and augmented versions—tends to yield better performance than when such samples are included. This further supports the idea that our augmentation strategy maintains meaningful feature relationships without introducing harmful inconsistencies.

APPENDIX K THEORETICAL ANALYSIS

Our self-training approach for malware detection under concept drift is theoretically supported by prior work on gradual self-training [39]. We outline key theoretical results explaining its effectiveness under distribution shifts, with commonly used notations summarized in Table XXII.

TABLE XXII: Summary of Notations

Notation	Description
P, Q	Source and target data distributions, respectively
P_t	Data distribution at time-step t
θ, θ'	Original and self-trained (updated) classifiers, respectively
Θ_R	Hypothesis class constrained by regularization parameter R
$\rho(P, Q)$	Wasserstein distance between distributions P and Q
ρ_m, ρ_b	Wasserstein distances for malware and benign classes
R	Regularization parameter
B	Upper bound on the norm of feature vectors
n	Number of unlabeled samples from target distribution
n_{τ_m, τ_b}	Number of samples retained after applying class-specific thresholds
α^*	Minimum achievable ramp loss on the target domain
α_0	Initial ramp loss on the source domain
$L_r(\theta, P)$	Ramp loss of classifier θ on distribution P
$L_r^m(\theta, P), L_r^b(\theta, P)$	Class-specific (malware and benign) ramp losses
q_m, q_b	Proportions of malware and benign samples ($q_m + q_b = 1$)
τ_m, τ_b	Confidence thresholds for malware and benign predictions, respectively
β	Error amplification factor, defined as $\frac{2}{1-\rho R}$.
δ	Confidence parameter for probabilistic bounds

A. Setup and Assumptions

We consider a gradual domain shift setting where we have a sequence of distributions P_0, P_1, \dots, P_T with P_0 as the source domain and P_T as the target domain. The shift is assumed to be gradual, meaning that for a small $\epsilon > 0$, the distance $\rho(P_t, P_{t+1}) < \epsilon$ for all $0 \leq t < T$, where ρ is a distributional distance metric.

We assume the existence of a sequence of classifiers θ_t that can classify most samples correctly with a margin and that the shift between consecutive domains is small enough to allow iterative adaptation.

B. Main Theoretical Results

The primary result from [39] states that under gradual domain shift, self-training can iteratively reduce error. Specifically:

Theorem 1 ([39], Theorem 3.2):

Let P and Q be two distributions such that the Wasserstein distance [66] satisfies $\rho(P, Q) = \rho < 1/R$, where R is the regularization parameter. Assume that both distributions have the same marginal distribution over labels, i.e., $P(Y) = Q(Y)$.

Suppose we have an initial model $\theta \in \Theta_R$ trained on P , and we perform self-training using n unlabeled samples from Q to obtain an updated model θ' . Then, with probability at least $1 - \delta$ over the sampling of n unlabeled examples from Q , the ramp loss [21] of the new model θ' on Q satisfies:

$$L_r(\theta', Q) \leq \frac{2}{1 - \rho R} L_r(\theta, P) + \alpha^* + \frac{4BR + \sqrt{2 \log(2/\delta)}}{\sqrt{n}}, \quad (6)$$

Here, $L_r(\theta, P)$ represents the ramp loss of the initial model on the source distribution P , while $\alpha^* = \min_{\theta^* \in \Theta_R} L_r(\theta^*, Q)$ denotes the minimum achievable ramp loss on the target distribution Q within the hypothesis space Θ_R . The term B is an upper bound on the norm of the input features, ensuring bounded feature magnitudes. The parameter R controls the capacity of the hypothesis space by regularizing the complexity of the learned models. Finally, δ is the confidence parameter that determines the probability with which the bound holds over the sampling of n unlabeled examples from Q .

This theorem implies that if the initial model has low loss on the source domain and the distributional shift is gradual, self-training will yield a model with controlled error on the new distribution. Applying this argument iteratively across T steps leads to an exponential improvement over direct adaptation:

Corollary 1 ([39], Corollary 3.3): Under the assumptions of α^* -separation, no label shift, gradual shift, and bounded data, suppose the initial model θ_0 has a ramp loss of at most $\alpha_0 \geq \alpha^*$ on the source distribution P_0 , i.e., $L_r(\theta_0, P_0) \leq \alpha_0$. If self-training is applied iteratively over T steps to produce the final model θ_T , denoted as $\theta_T = ST(\theta_0, (S_1, \dots, S_T))$, then with high probability, the ramp loss on the final target distribution P_T is bounded as:

$$L_r(\theta_T, P_T) \leq \beta^{T+1} \left(\alpha_0 + \frac{4BR + \sqrt{2 \log(2T/\delta)}}{\sqrt{n}} \right) \quad (7)$$

where $\beta = \frac{2}{1 - \rho R}$. This result demonstrates that gradual self-training effectively controls the error over multiple adaptation steps, preventing the potential failure cases that can arise from direct adaptation.

C. Extension to ADAPT

In the malware classification setting, we extend the theoretical framework by considering different distribution shifts for the two classes: malware and benign. Let ρ_m and ρ_b denote the Wasserstein shifts for the malware and benign classes, respectively, where we assume $\rho_m > \rho_b$. This reflects the practical scenario where malware samples undergo more significant distributional changes compared to benign samples.

1) *Asymmetric Error:* Following Lemma A.2 from [39], we analyze the classification error for each class separately under these different shift magnitudes. The classification error on the target distribution Q for malware and benign classes can be bounded as:

$$\begin{aligned} \text{Err}^m(\theta, Q) &\leq \frac{1}{1 - \rho_m R} L_r^m(\theta, P), \\ \text{Err}^b(\theta, Q) &\leq \frac{1}{1 - \rho_b R} L_r^b(\theta, P). \end{aligned} \quad (8)$$

Since $\rho_m > \rho_b$, it follows that the multiplicative factor $\frac{1}{1 - \rho_m R}$ is larger than $\frac{1}{1 - \rho_b R}$. This implies that, even if the initial ramp losses $L_r^m(\theta, P)$ and $L_r^b(\theta, P)$ were similar, the resulting classification error for malware will be higher than that for benign samples under distribution shift.

A direct consequence of this is that malware samples, experiencing a greater shift, are more likely to be pushed toward the benign decision region than the reverse. Since errors occur primarily when samples cross the decision boundary, a higher shift for malware leads to more malware samples being misclassified as benign, increasing the false negative rate (FNR). In contrast, the smaller shift ρ_b for benign samples means fewer of them cross into the malware region, resulting in a lower false positive rate (FPR). Thus, the asymmetry in shift magnitudes naturally leads to FNR exceeding FPR, explaining the observed trend in malware classification under distribution shift.

2) *Impact of Class-Specific Thresholding:* To mitigate the imbalance between false negative and false positive rates, we introduce separate thresholds τ_m and τ_b for malware and benign classifications, respectively. Instead of classifying all samples, we only classify those for which the model's confidence exceeds the respective threshold. This effectively reduces the number of classified samples but also lowers the classification error.

Formally, let $Q_{\tau_m}^m$ and $Q_{\tau_b}^b$ denote the distributions of malware and benign samples that remain after thresholding. Since thresholding removes uncertain samples near the decision boundary, the ramp loss on the remaining classified samples decreases:

$$\begin{aligned} L_r^m(\theta, Q_{\tau_m}^m) &\leq L_r^m(\theta, Q), \\ L_r^b(\theta, Q_{\tau_b}^b) &\leq L_r^b(\theta, Q). \end{aligned} \quad (9)$$

Applying the error bound from Equation (8) to the thresholded samples, we obtain:

$$\begin{aligned}\text{Err}^m(\theta, Q) &\leq \frac{1}{1 - \rho_m R} L_r^m(\theta, P_{\tau_m}), \\ \text{Err}^b(\theta, Q) &\leq \frac{1}{1 - \rho_b R} L_r^b(\theta, P_{\tau_b}).\end{aligned}\quad (10)$$

Since thresholding removes samples that are close to the decision boundary—where errors are more likely—the filtered distributions $Q_{\tau_m}^m$ and $Q_{\tau_b}^b$ contain fewer misclassified samples, leading to lower classification errors.

Thresholding reduces the number of classified samples, which affects the generalization bound in Equation (6). Specifically, the third term in the bound, which depends on the sample size n , is modified as follows:

$$\frac{4BR + \sqrt{2\log(2/\delta)}}{\sqrt{n}} \rightarrow \frac{4BR + \sqrt{2\log(2/\delta)}}{\sqrt{n_{\tau_m, \tau_b}}}, \quad (11)$$

where n_{τ_m, τ_b} is the number of samples retained after thresholding at τ_m and τ_b , and we have $n_{\tau_m, \tau_b} < n$. Since the denominator decreases, this term increases, leading to a looser bound.

3) *Modified Error Bound:* Following Lemma A.3 from [39], we account for the fact that the total error depends on the mixture of malware and benign samples in Q . Given that q_m and q_b represent the proportions of malware and benign samples in Q (i.e., $q_m + q_b = 1$), we replace the expectation in the bound with an explicit weighted sum.

First, the error term in Equation (6) becomes:

$$\begin{aligned}\frac{2}{1 - \rho R} L_r(\theta, P) &\rightarrow q_m \frac{2}{1 - \rho_m R} L_r^m(\theta, P_{\tau_m}) \\ &\quad + q_b \frac{2}{1 - \rho_b R} L_r^b(\theta, P_{\tau_b}).\end{aligned}\quad (12)$$

Thus, the final modified bound becomes:

$$\begin{aligned}L_r(\theta', Q_{\tau_m, \tau_b}) &\leq q_m \frac{2}{1 - \rho_m R} L_r^m(\theta, P_{\tau_m}) \\ &\quad + q_b \frac{2}{1 - \rho_b R} L_r^b(\theta, P_{\tau_b}) \\ &\quad + \alpha^* \\ &\quad + \frac{4BR + \sqrt{2\log(2/\delta)}}{\sqrt{n_{\tau_m, \tau_b}}}.\end{aligned}\quad (13)$$

The modified bound in Equation (13) reduces to the original bound in Equation (6) when the distribution shifts for both classes are identical ($\rho_m = \rho_b = \rho$) and all samples are selected after thresholding, i.e., no data is filtered ($Q_{\tau_m, \tau_b} = Q$, $n_{\tau_m, \tau_b} = n$).

4) *Impact of Augmentation & Mixup:* Data augmentation and mixup have been shown to act as regularizers during training [41], [76], effectively reducing overfitting. This regularization effect leads to a decrease in the bound given in Equation 13. Specifically, stronger regularization implicitly reduces the norm of the learned weight vector w , which corresponds

to a smaller R in our formulation (i.e., enforcing $\|w\|_2 \leq R$). A smaller R limits the model's capacity, preventing it from fitting noise or learning overly complex decision boundaries. As a result, stronger regularization (smaller R) tightens the bound and enhances robustness to distribution shifts. We leave a precise theoretical analysis of these effects for future work.

APPENDIX L HYPERPARAMETER SEARCH

We present the range of hyperparameters used for different methods in Table XXIII. For self-training baselines, we adopt the default parameters for the five online learning classifiers used in our experiments. Insomnia, MORSE, and our proposed method ADAPT utilize different underlying machine learning models. Specifically, Insomnia employs a co-training approach with XGBoost and MLP, while MORSE uses MLP. In contrast, we evaluate ADAPT with Random Forest, XGBoost, and MLP. The same parameter search space is applied for these models as in the offline learning setup. We conduct a random search of 200 trials within the joint search space (i.e., combining classifier-specific and self-training-specific parameters) to select the best hyperparameters for all datasets.

TABLE XXIII: Hyperparameter search spaces for various methods. "U" indicates sampling from a uniform random distribution within the specified range. Hyperparameters marked with "*" are only used during the retraining phase. The Insomnia method also uses hyperparameters from MLP and XGBoost, while MORSE uses those from MLP. ADAPT utilizes the baseline model, which can be either Random Forest (RF), XGBoost, or MLP.

Model	Hyperparameter	Candidate Values
Random Forest	n_estimators	2^x , where $x \in \mathcal{U}[5, 10]$
	max_depth	2^y , where $y \in \mathcal{U}[5, 10]$
	criterion	{gini, entropy, log_loss}
	class_weight	{None, "balanced"}
XGBoost	max_depth	2^w , where $w \in \mathcal{U}[3, 7]$
	alpha	10^a , where $a \in \mathcal{U}[-8, 0]$
	lambda	10^b , where $b \in \mathcal{U}[-8, 0]$
	eta	3.0×10^c , where $c \in \mathcal{U}[-2, -1]$
	balance	{True, False}
	num_boost_round	{100, 150, 200, 300, 400}
MLP	mlp_layers	{[100, 100], [512, 256, 128], [512, 384, 256, 128], [512, 384, 256, 128, 64]}
	learning_rate	10^d , where $d \in \mathcal{U}[-5, -3]$
	dropout	x , where $x \in \mathcal{U}[0.0, 0.5]$
	batch_size	2^e , where $e \in \{5, 6, 7, 8, 9, 10\}$
	epochs	{25, 30, 35, 40, 50, 60, 80, 100, 150}
	optimizer	{Adam}
	balance	{True, False}
	cont_learning_epochs*	{0.1, 0.2, 0.3, 0.4, 0.5}
SVM	C	10^z , where $z \in \mathcal{U}[-4, 3]$
	class_weight	{None, "balanced"}
ARF	n_models	2^x , where $x \in \mathcal{U}[3, 5]$
	max_features	{sqrt, log2, None}
	max_depth	2^y , where $y \in \mathcal{U}[5, 10]$
	lambda_value	6
	threshold	x , where $x \in \mathcal{U}[0.6, 0.99]$
DE++	age_threshold_low	x , where $x \in \mathcal{U}[0.0, 0.5]$
	buffer_ratio	x , where $x \in \mathcal{U}[0.1, 0.5]$
	buffer_size	{1000, 2000, 3000}
Insomnia	fraction	x , where $x \in \mathcal{U}[0.0, 0.8]$
MORSE	threshold	x , where $x \in \mathcal{U}[0.8, 0.99]$
	weak_augment	x , where $x \in \mathcal{U}[0.0, 0.1]$
	strong_augment	x , where $x \in \mathcal{U}[0.1, 0.2]$
ADAPT	threshold_benign	x , where $x \in \mathcal{U}[0.8, 0.99]$
	threshold_malware	x , where $x \in \mathcal{U}[0.6, 0.99]$
	lambda	x , where $x \in \mathcal{U}[0.0, 0.5]$
	mask_ratio	x , where $x \in \mathcal{U}[0.0, 0.2]$
	mixup_alpha	x , where $x \in \mathcal{U}[0.0, 0.2]$